

Phase-dependent absorption features in X-ray spectra of XDINS

Alice Borghese

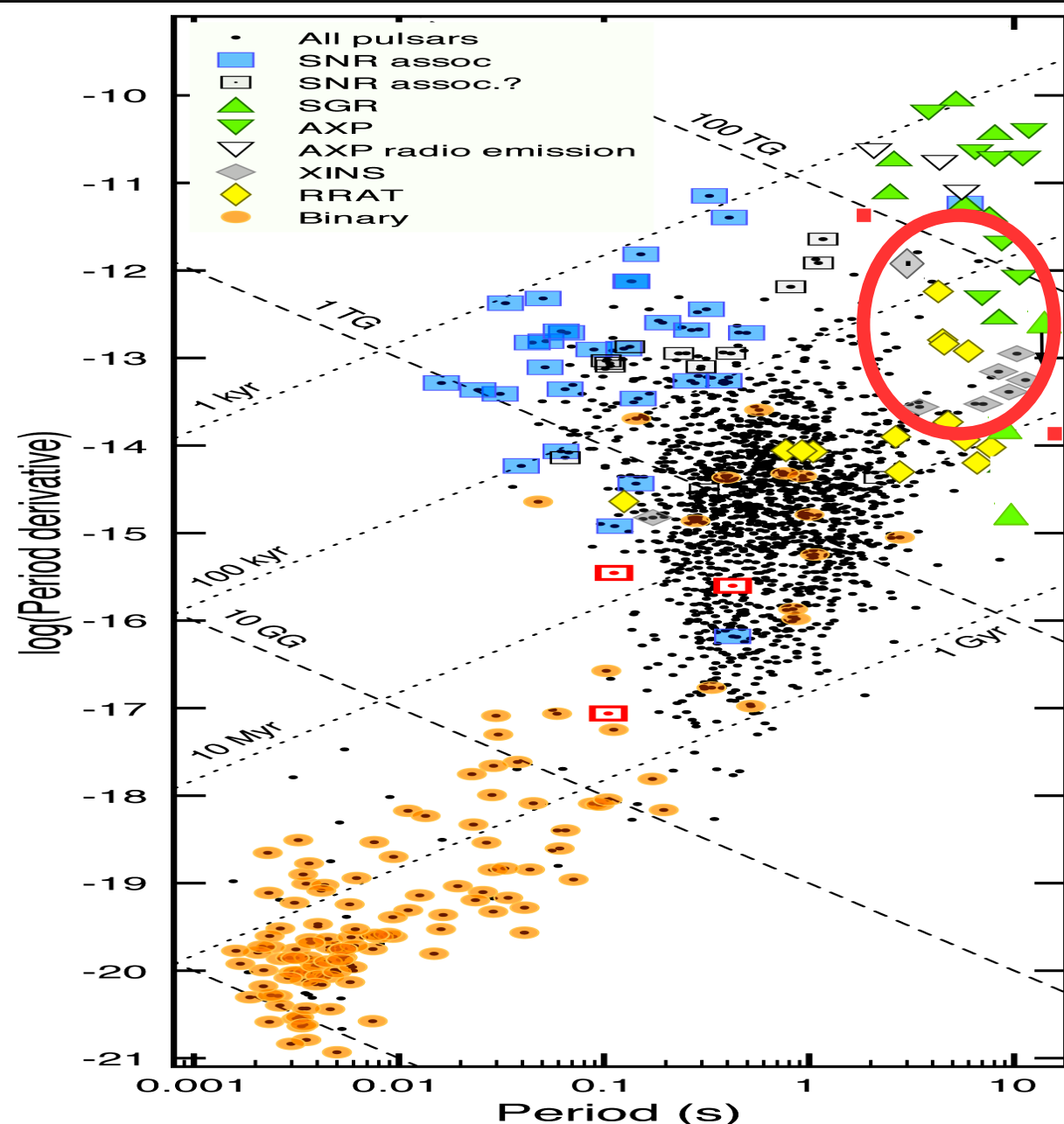
Anton Pannekoek Institute for Astronomy, University of Amsterdam

In collaboration with N. Rea (U. Amsterdam, CSIC-IEEC),
F. Coti Zelati (CSIC-IEEC), A. Tiengo (IUSS, INAF), R. Turolla (U.
Padua, MSSL), S. Zane (MSSL)

Borghese et al., 2015, ApJ, 807, L20
Borghese et al., 2017, MNRAS, 468, 2975



THE SAMPLE: X-ray Dim Isolated Neutron stars (XDINSs)



Distance: $d \lesssim 500$ pc

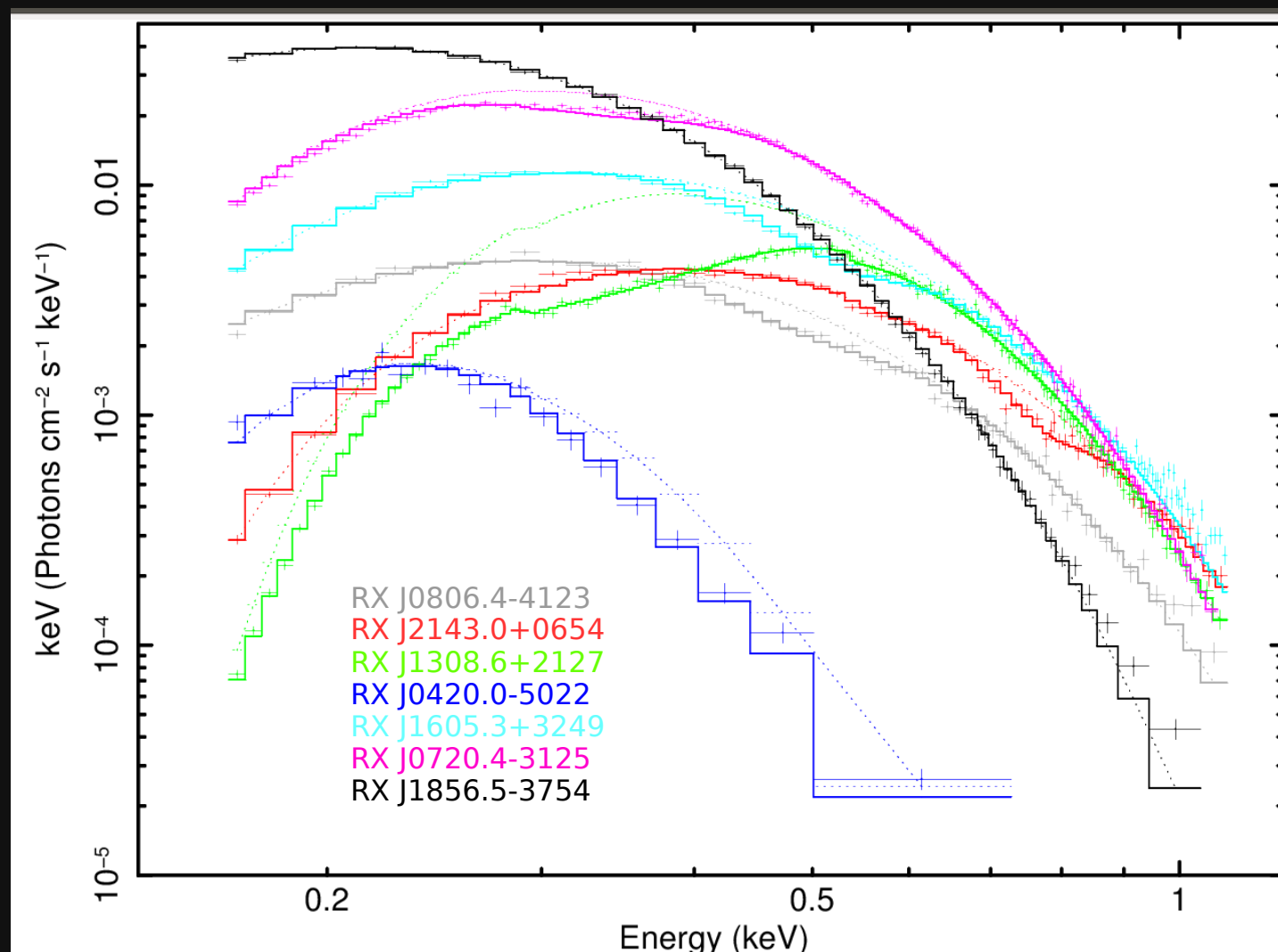
Spin period: $P \sim 3 - 11$ s

Magnetic field: $B_{\text{dip}} \approx 10^{13}$ G

Age: $\tau_c \approx 10^6$ yr

Luminosity: $L_x \approx 10^{31-32}$ erg s⁻¹

Image credit: C. M. Espinoza



Thermal X-ray spectra:
 $kT_{\text{BB}} \approx 50-100 \text{ eV}$

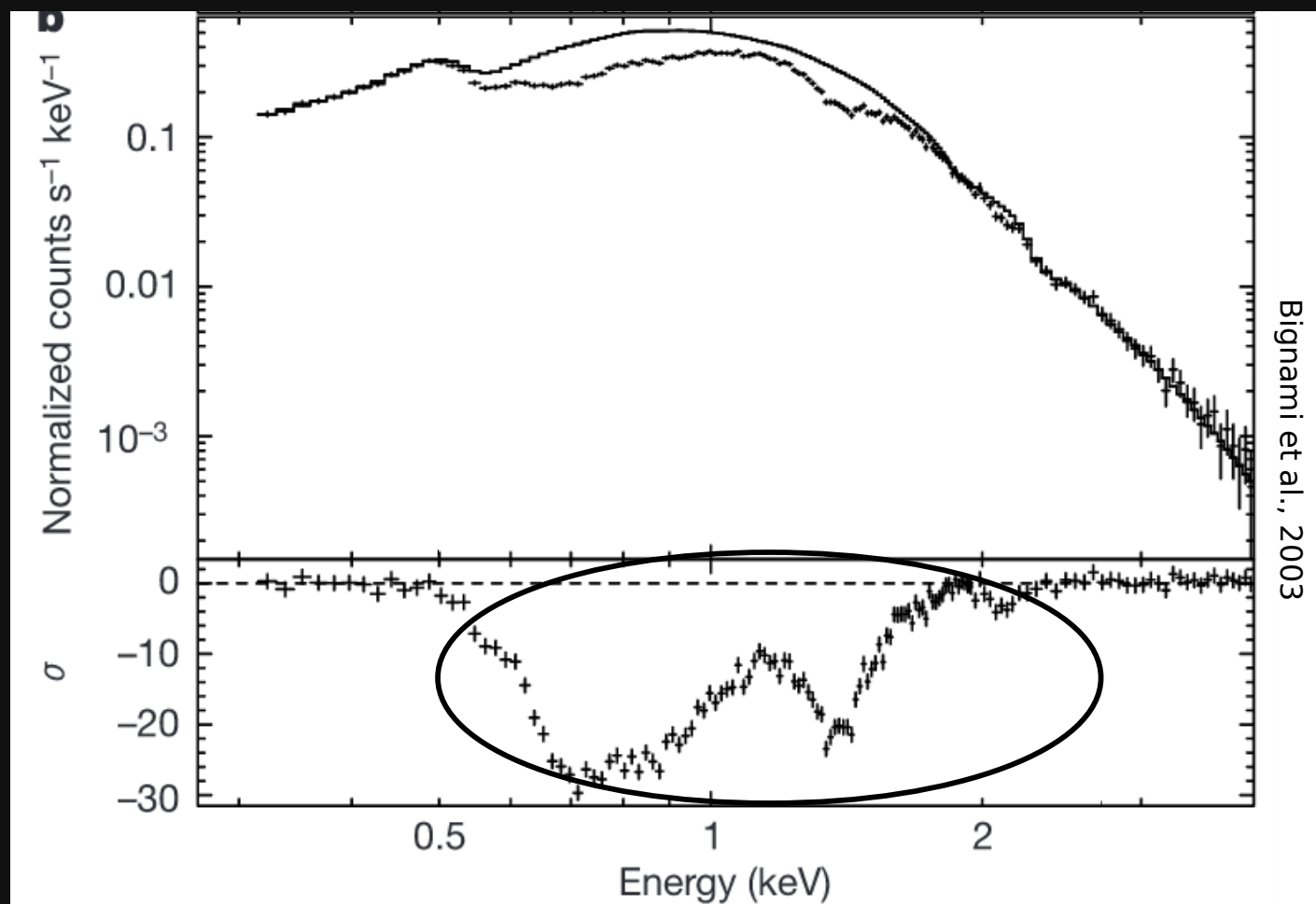
plus a broad absorption
feature:
 $E_{\text{line}} \approx 0.2-0.8 \text{ keV}$

Origin of the broad features:

1. proton cyclotron resonances/atomic transitions (van Kerkwijk & Kaplan, 2006)
2. inhomogeneous surface temperature distribution (Viganó et al., 2014)

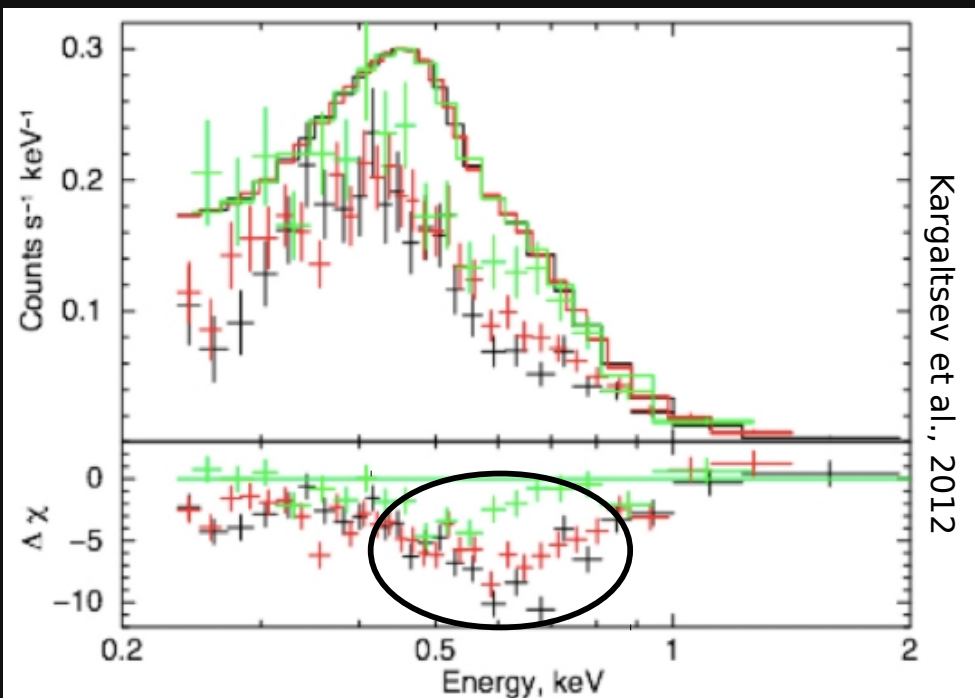
CCO

1E 1207.4-5209
 $E_{\text{line}} \sim 0.7, 1.4, 2.1 \text{ keV}$



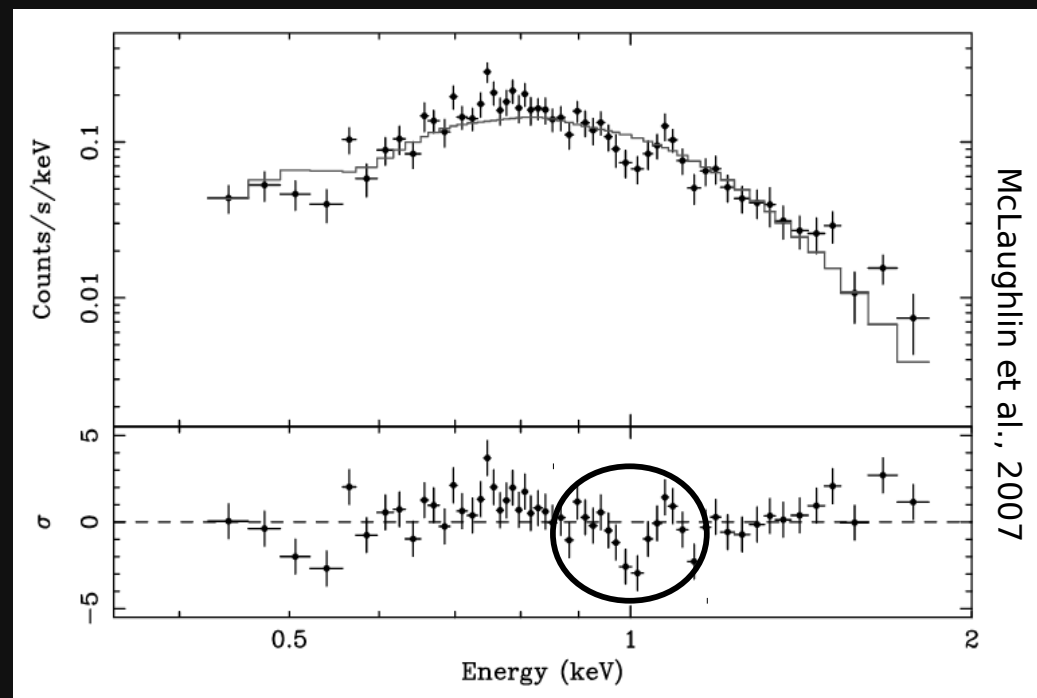
RADIO PULSARS

PSR J1740+1000
 $E_{\text{line}} \sim 0.6 \text{ keV}$

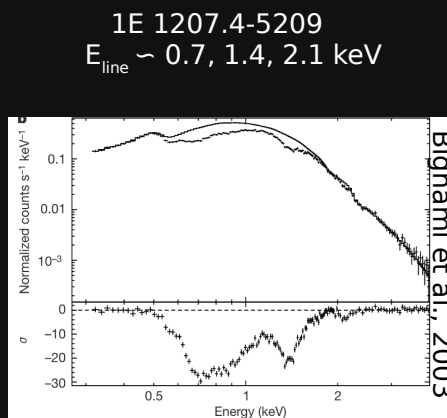
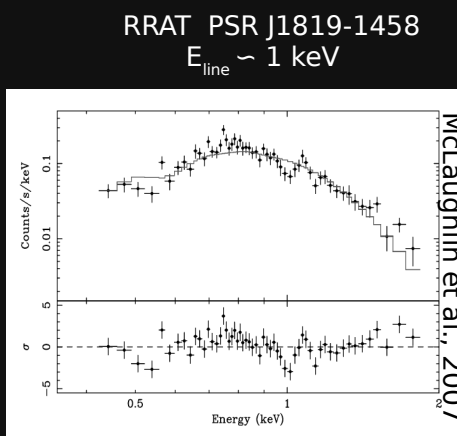
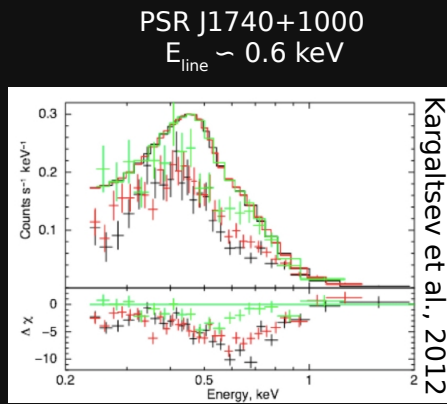


Kargaltsev et al., 2012

RRAT PSR J1819-1458
 $E_{\text{line}} \sim 1 \text{ keV}$

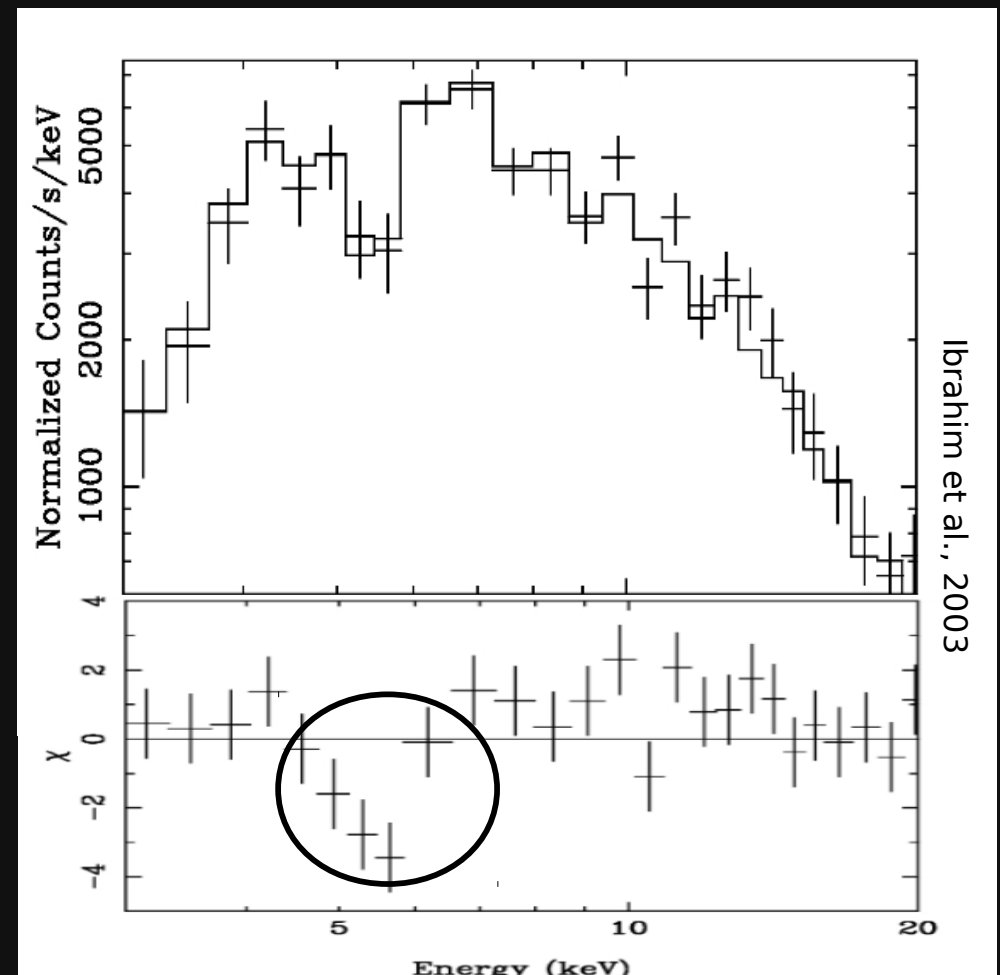


McLaughlin et al., 2007



MAGNETARS

SGR J1806-20 $E_{\text{line}} \sim 5 \text{ keV}$



Other claims

- 1RXS J170849-400910: $E_{\text{line}} \sim 8 \text{ keV}$ (Rea et al., 2003)
- XTE J1810-197: $E_{\text{line}} \sim 1.1 \text{ keV}$ (Bernardini et al., 2009)

need confirmation

LOW MAGNETIC FIELD MAGNETARS

SGR 0418+5729

$$E_{\text{line}} \gtrsim 2 \text{ keV}$$

$$B_{\text{dip}} = 6 \times 10^{12} \text{ G}$$

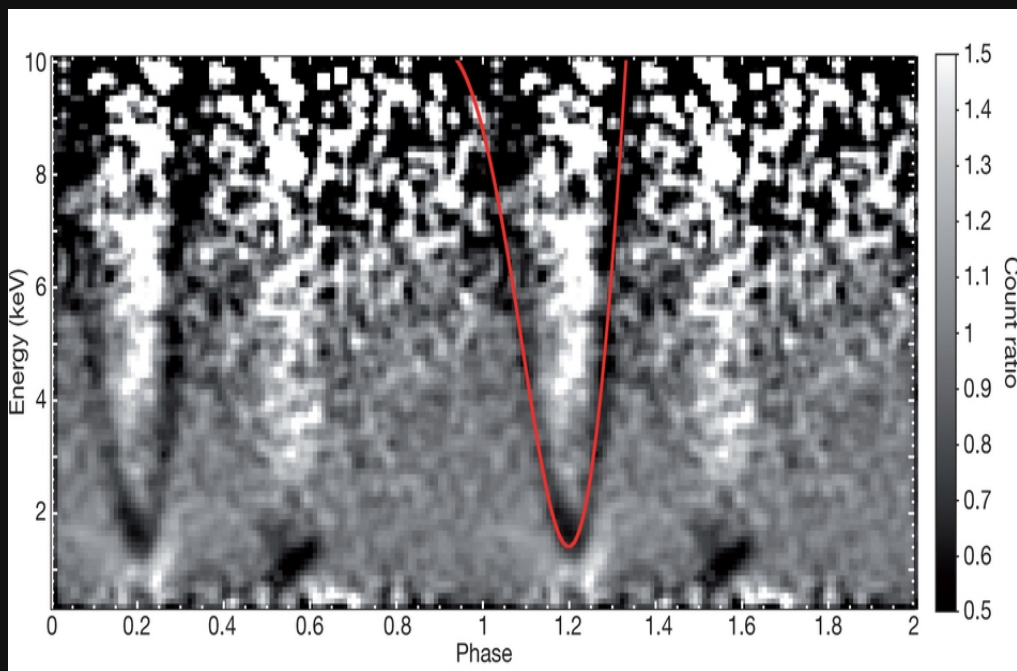
Proton cyclotron scattering
 $\rightarrow B > 2 \times 10^{14} \text{ G}$

SWIFT J1822.3-1606

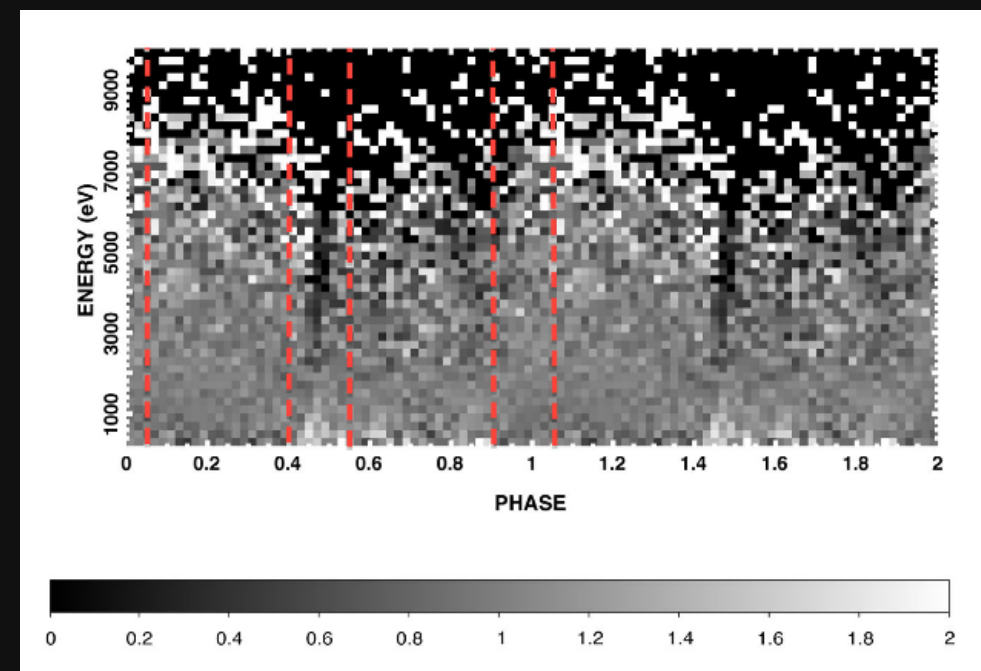
$$E_{\text{line}} \sim 6.5 \text{ keV}$$

$$B_{\text{dip}} = 3.4 \times 10^{13} \text{ G}$$

Proton cyclotron scattering
 $\rightarrow B > 10^{14} \text{ G}$

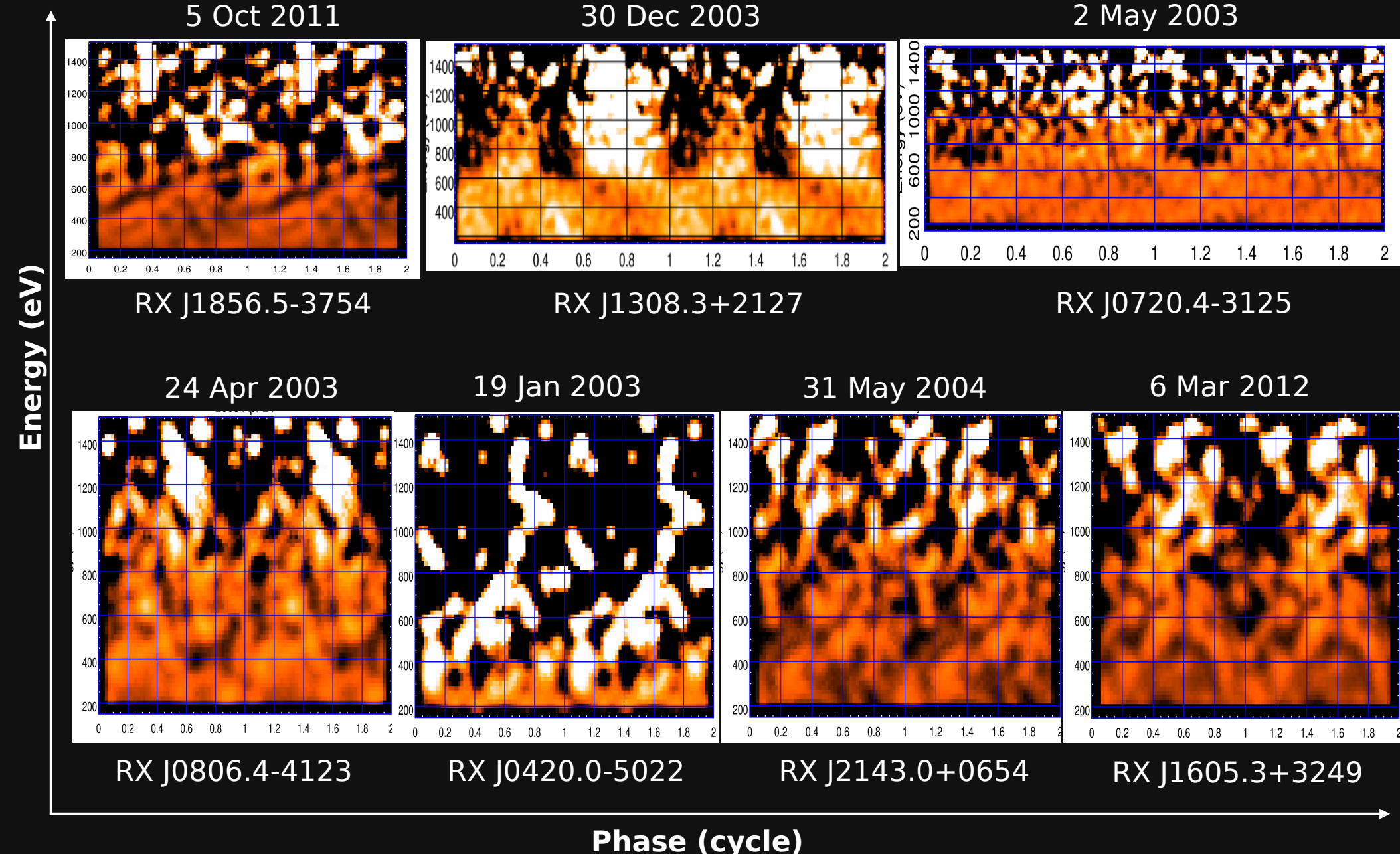


Tiengo et al., 2013



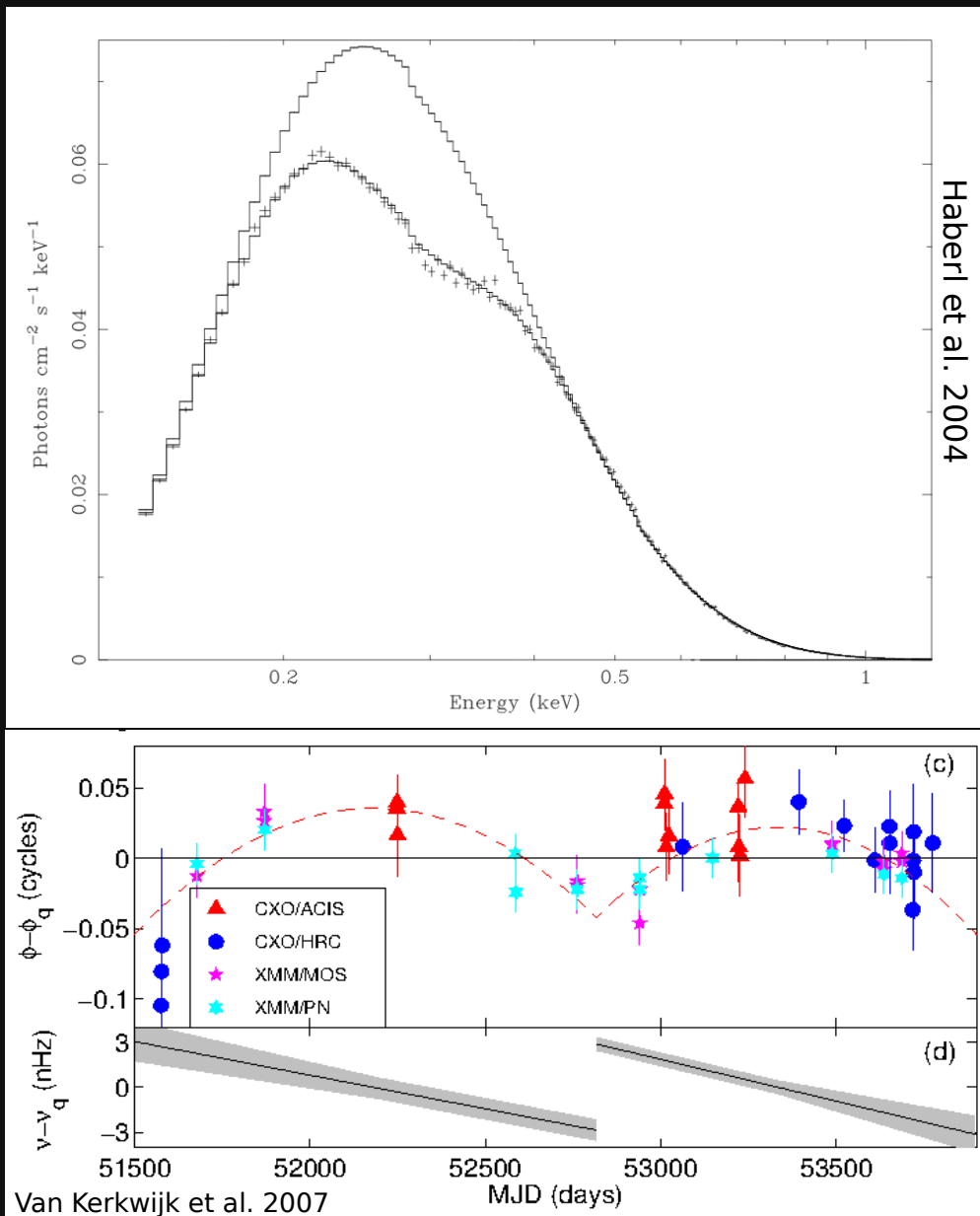
Rodriguez Castillo et al., 2016

SEARCHING FOR NARROW PHASE-DEPENDENT FEATURES



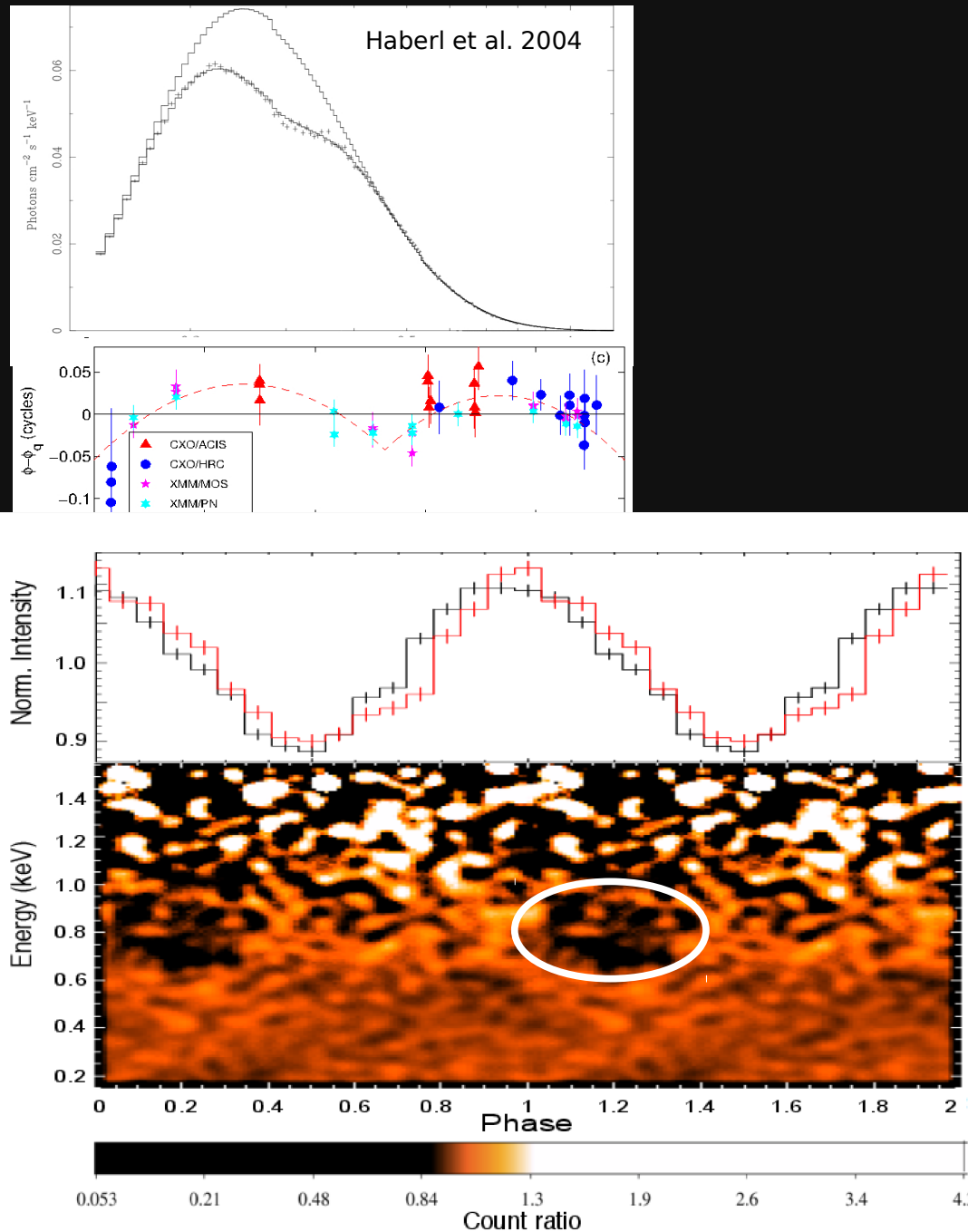
Borghese et al., 2017, MNRAS

RX J0720.4-3125: General properties



- Spin period $P = 8.39$ s
- Dipolar magnetic field: $B_{\text{dip}} \sim 2.5 \times 10^{13}$ G
- Black body spectrum plus a broad absorption feature ($E_{\text{line}} \sim 270$ eV, $\sigma \sim 65$ eV, $kT_{\text{BB}} \sim 85$ eV)
- Long-term variations in timing and spectral parameters (possibly due to a glitch)
- Pulsed Fraction: 11%

RX J0720.4-3125: General properties



- Spin period $P = 8.39$ s
- Dipolar magnetic field: $B_{\text{dip}} \sim 2.5 \times 10^{13}$ G
- Black body spectrum plus a broad absorption feature ($E_{\text{line}} \sim 270$ eV, $\sigma \sim 65$ eV, $kT_{\text{BB}} \sim 85$ eV)
- Long-term variations in timing and spectral parameters (possibly due to a glitch)
- Pulsed Fraction: 11%

red: May 2nd, 2003 observation (51 ks)

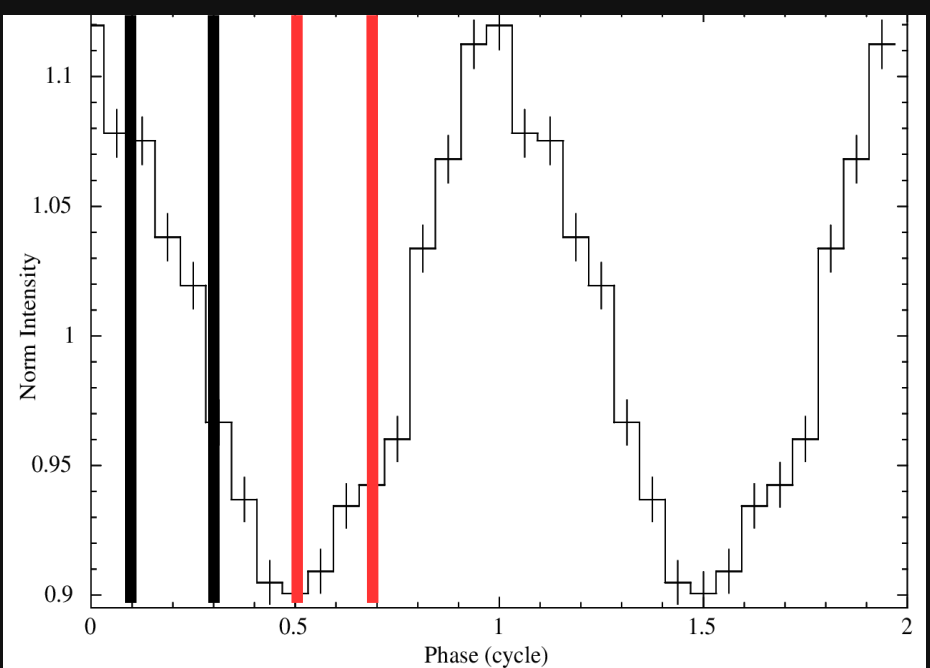
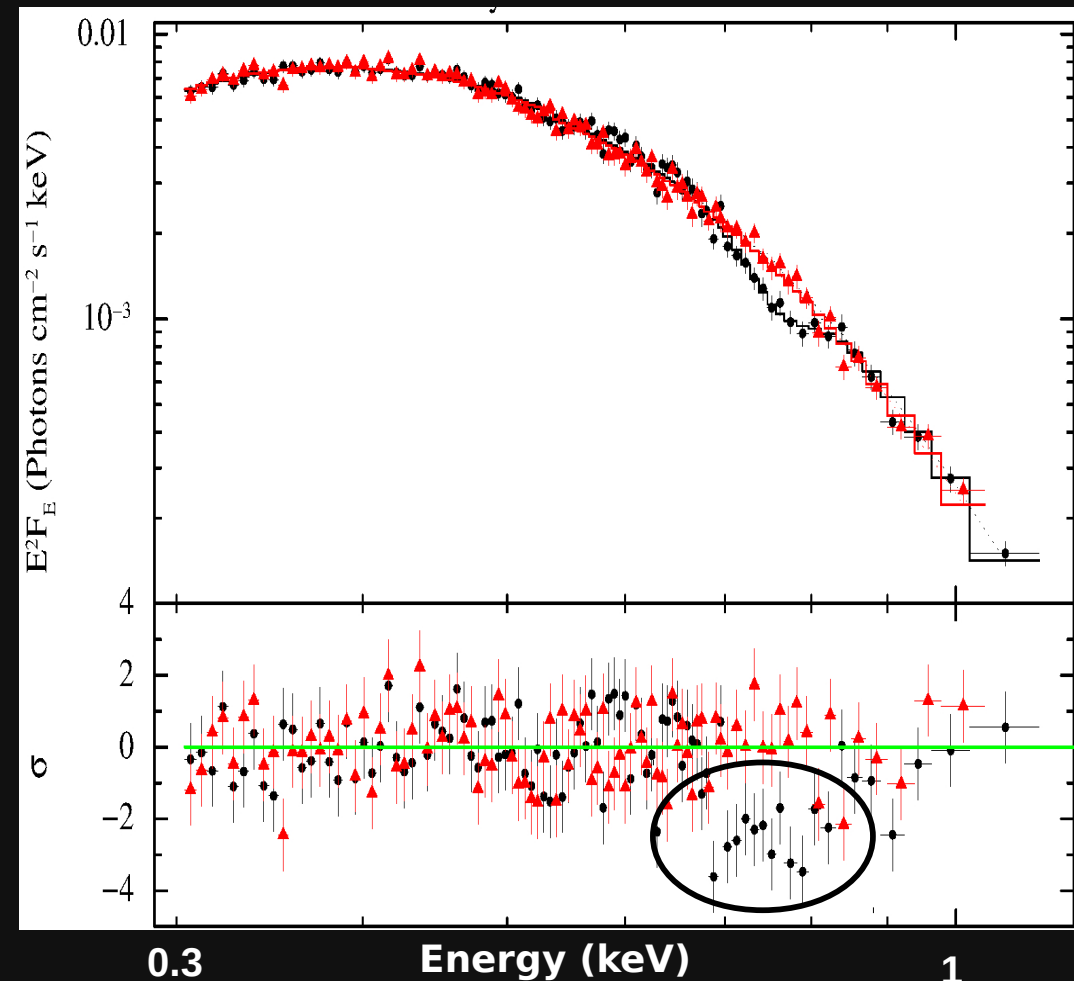
black: combined spectrum (407 ks)

An additional narrow phase-dependent spectral feature is present.

Borghese et al., 2015, ApJL

RX J0720.4-3125: Phase-Resolved spectral analysis





Phase-dependent line:

$$E_{\text{line}} = 745 {}^{+17}_{-27} \text{ eV}$$

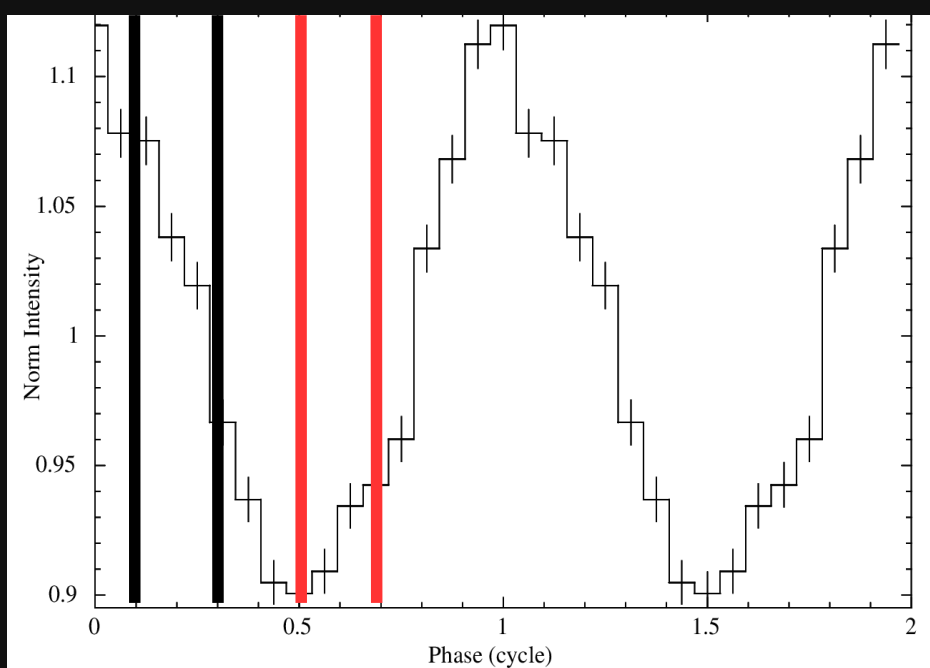
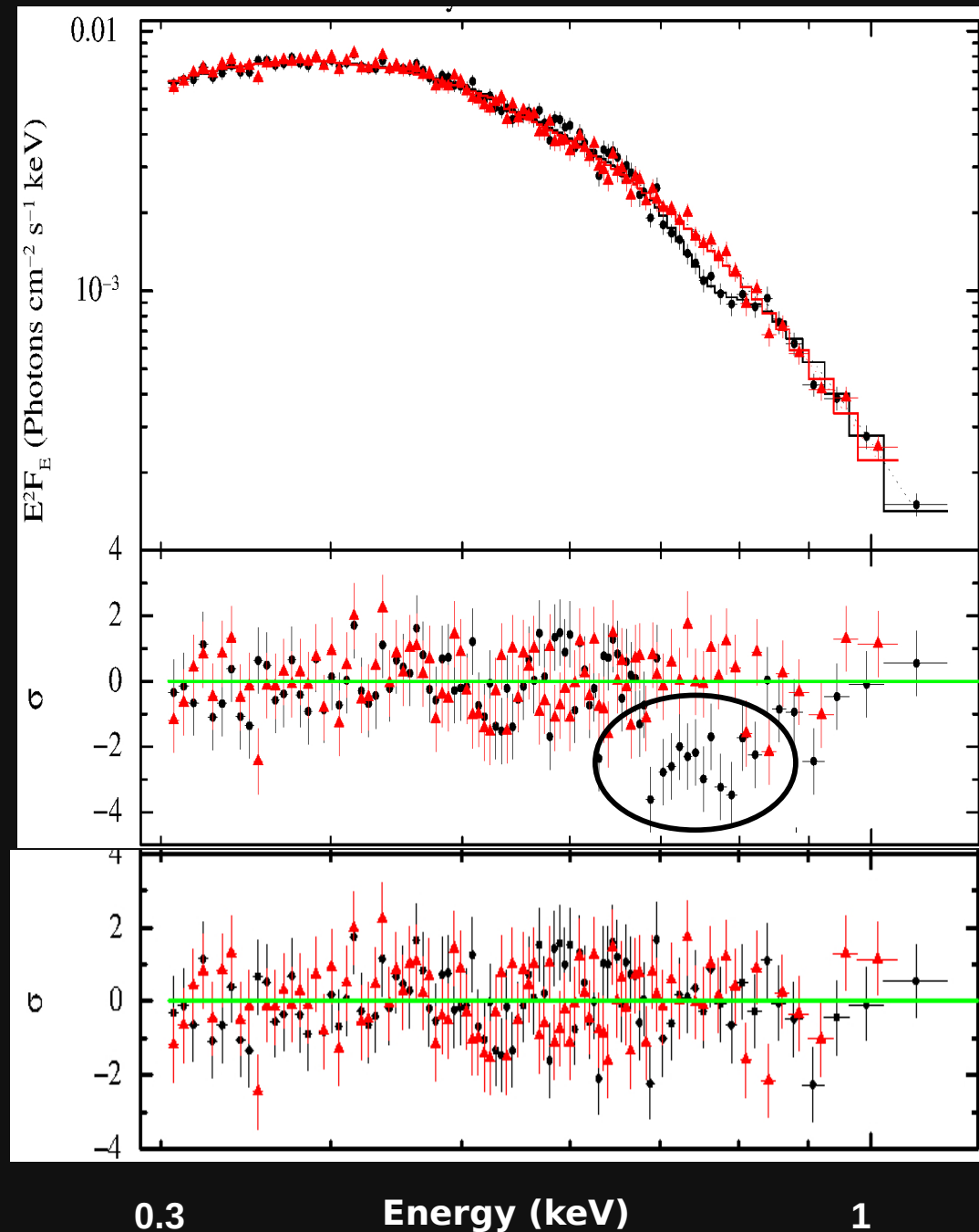
$$\sigma_{\text{line}} = 42 {}^{+51}_{-33} \text{ eV}$$

$$\text{Eqw} = 28 {}^{+9}_{-11} \text{ eV}$$

F-test significance $\sim 5\sigma$

Borghese et al., 2015, ApJL

RX J0720.4-3125: Phase-Resolved spectral analysis



Phase-dependent line:

$$E_{\text{line}} = 745 {}^{+17}_{-27} \text{ eV}$$

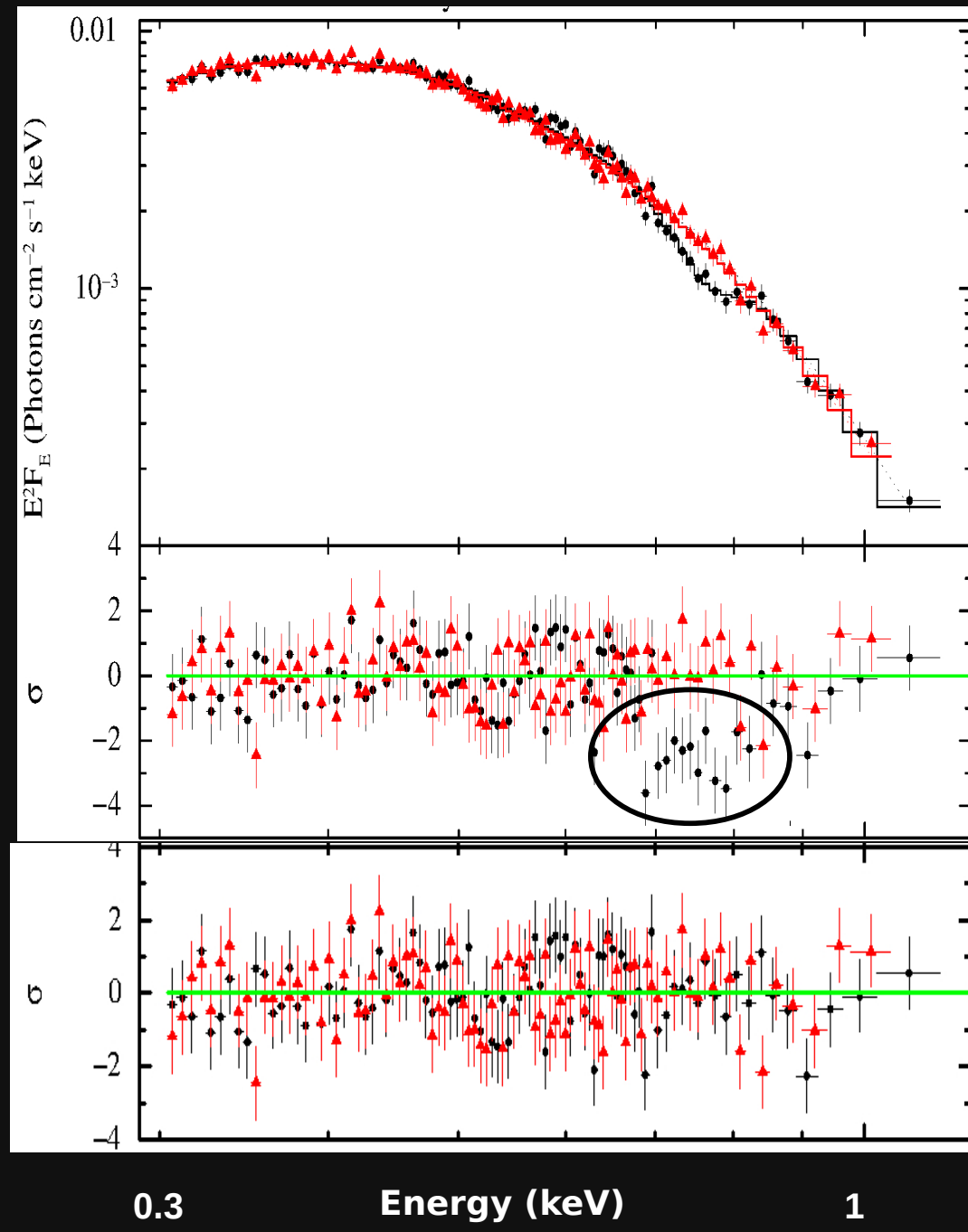
$$\sigma_{\text{line}} = 42 {}^{+51}_{-33} \text{ eV}$$

$$\text{Eqw} = 28 {}^{+9}_{-11} \text{ eV}$$

F-test significance $\sim 5\sigma$

Borghese et al., 2015, ApJL

RX J0720.4-3125: Phase-Resolved spectral analysis

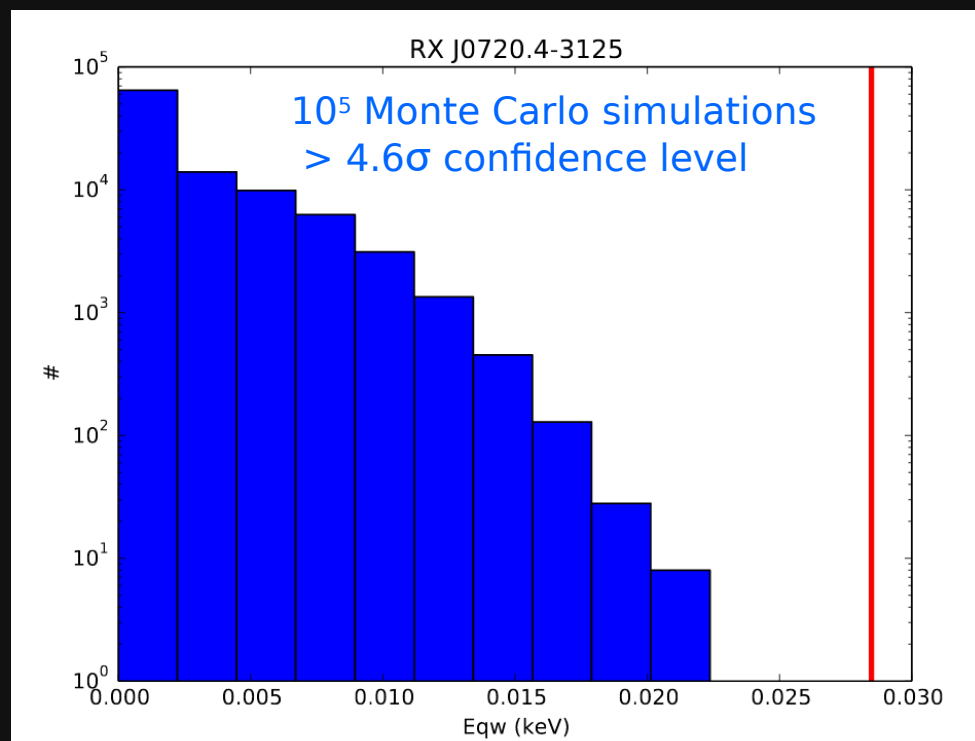


Phase-dependent line:

$$E_{\text{line}} = 745 {}^{+17}_{-27} \text{ eV}$$

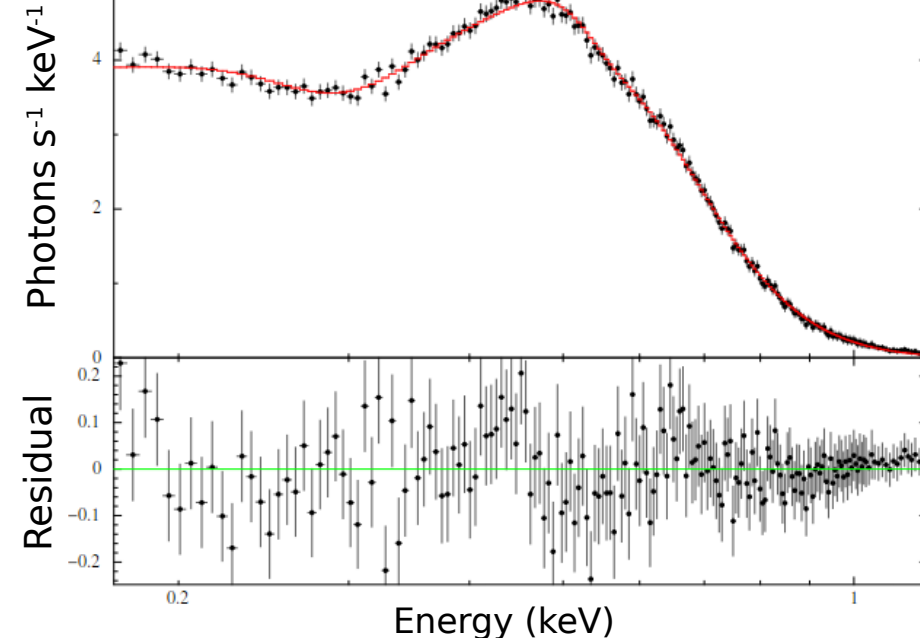
$$\sigma_{\text{line}} = 42 {}^{+51}_{-33} \text{ eV}$$

$$\text{Eqw} = 28 {}^{+9}_{-11} \text{ eV}$$



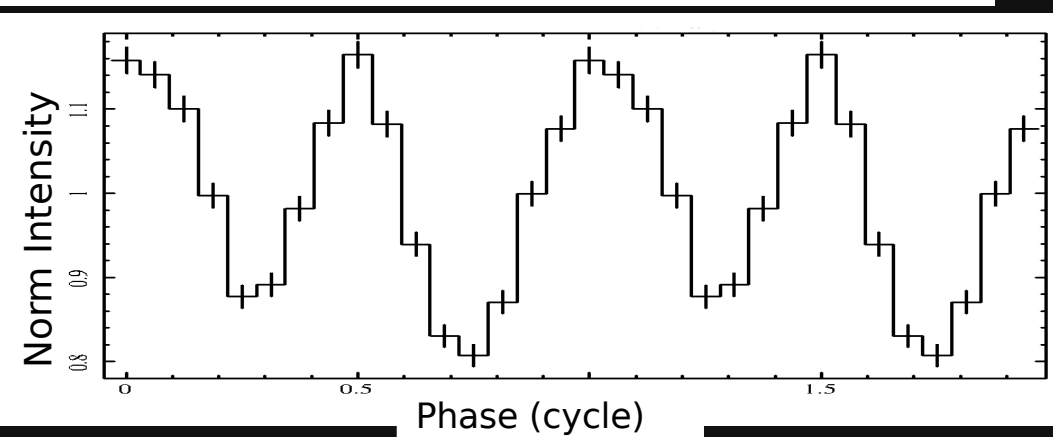
Borghese et al., 2015, ApJL; 2017, MNRAS

RX J1308.6+2127: General properties

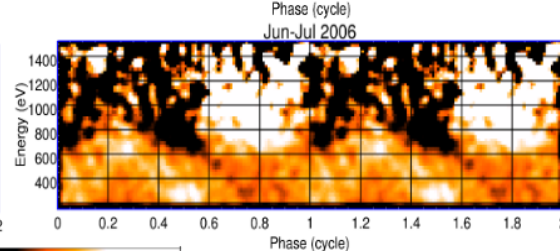
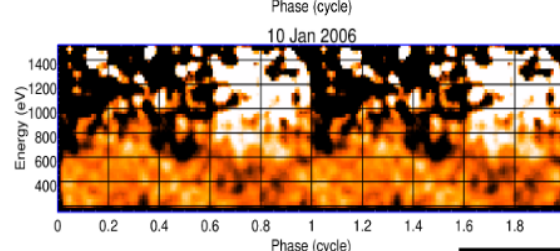
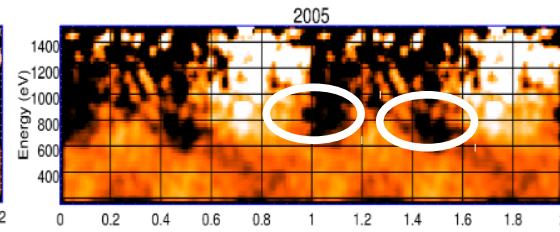
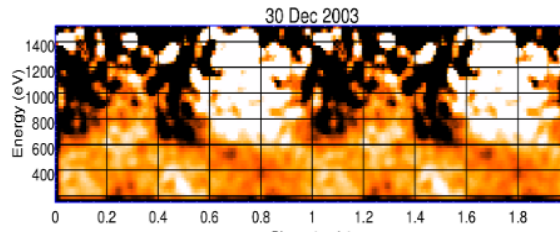
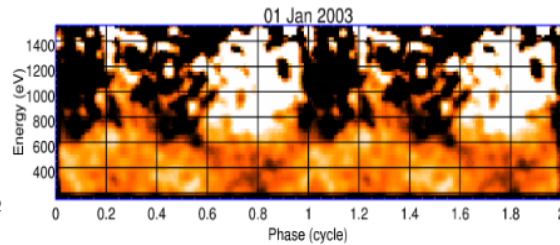
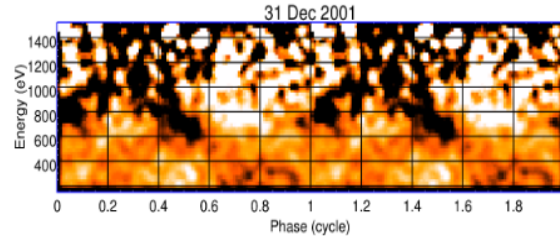
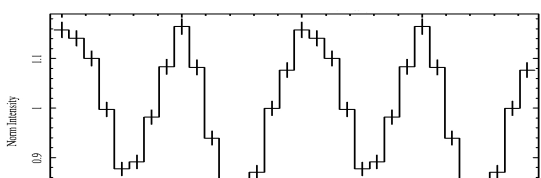
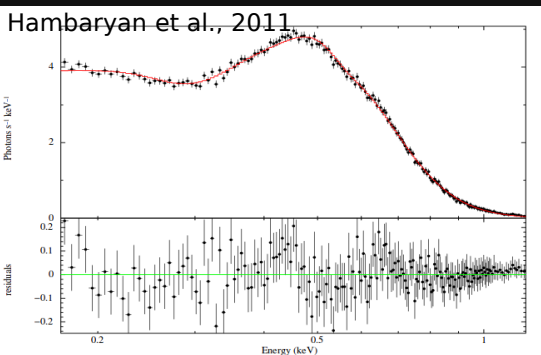


Hambaryan et al., 2011

- Spin period P = 10.31 s
- Dipolar magnetic field: $B_{\text{dip}} \sim 3.4 \times 10^{13}$ G
- Black body spectrum plus a broad absorption feature ($E_{\text{line}} \sim 270$ eV, $\sigma \sim 155$ eV, $kT_{\text{BB}} \sim 86$ eV)
- Double-humped pulse profile
- Pulsed Fraction: 19%



RX J1308.6+2127: General properties

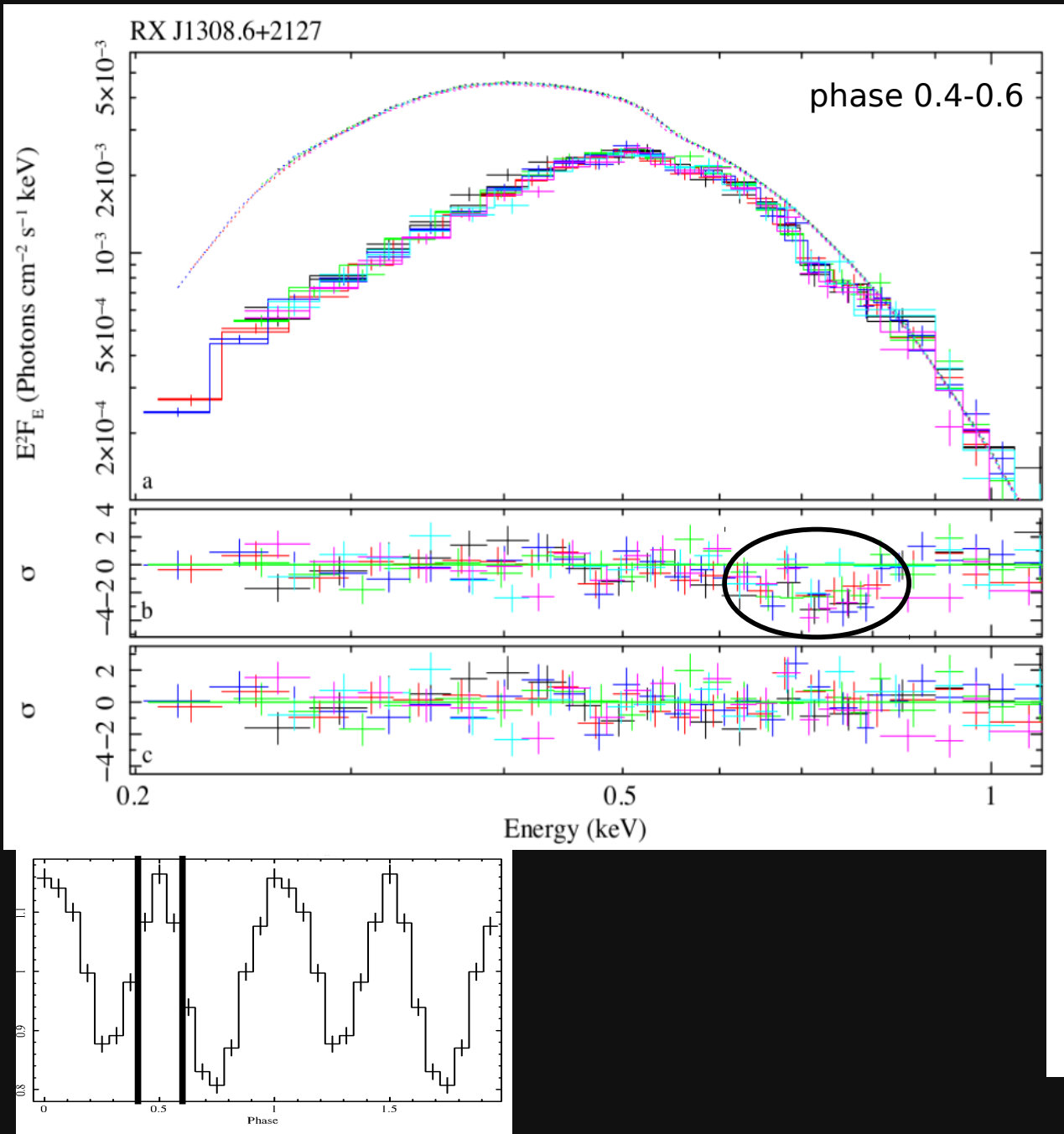


0.47 0.74 1.1 1.5
Count Ratio

- Spin period $P = 10.31 \text{ s}$
- Dipolar magnetic field: $B_{\text{dip}} \sim 3.4 \times 10^{13} \text{ G}$
- Black body spectrum plus a broad absorption feature ($E_{\text{line}} \sim 270 \text{ eV}$, $\sigma \sim 155 \text{ eV}$, $kT_{\text{BB}} \sim 86 \text{ eV}$)
- Double-humped pulse profile
- Pulsed Fraction: 19%

All available XMM-Newton observations show an additional narrow spectral feature in certain rotational phases.

RX J1308.6+2127: Phase-Resolved spectral analysis

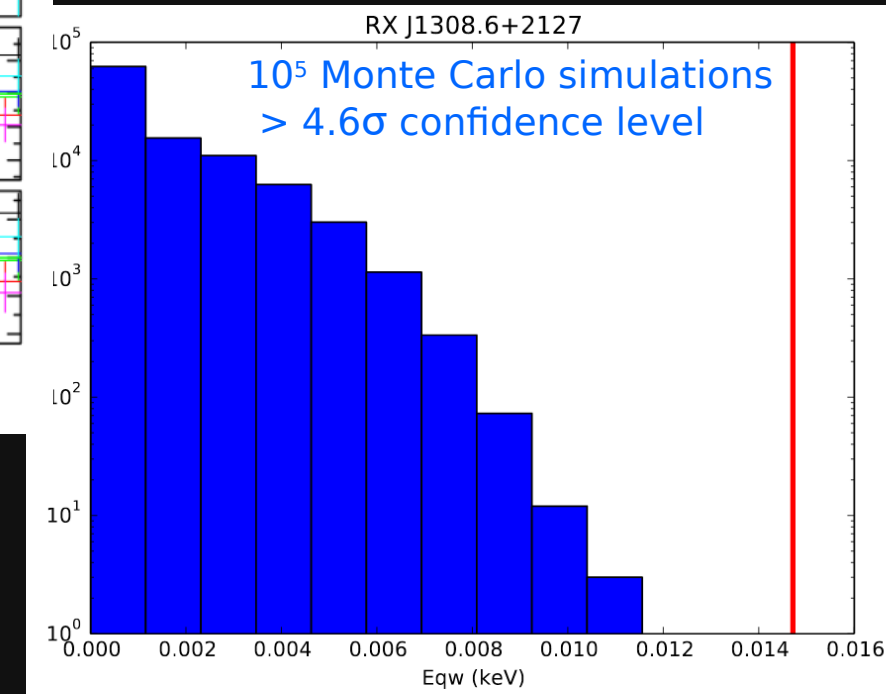


Phase-dependent line:

$$E_{\text{line}} = 736^{+18}_{-16} \text{ eV}$$

σ_{line} compatible with the spectral energy resolution

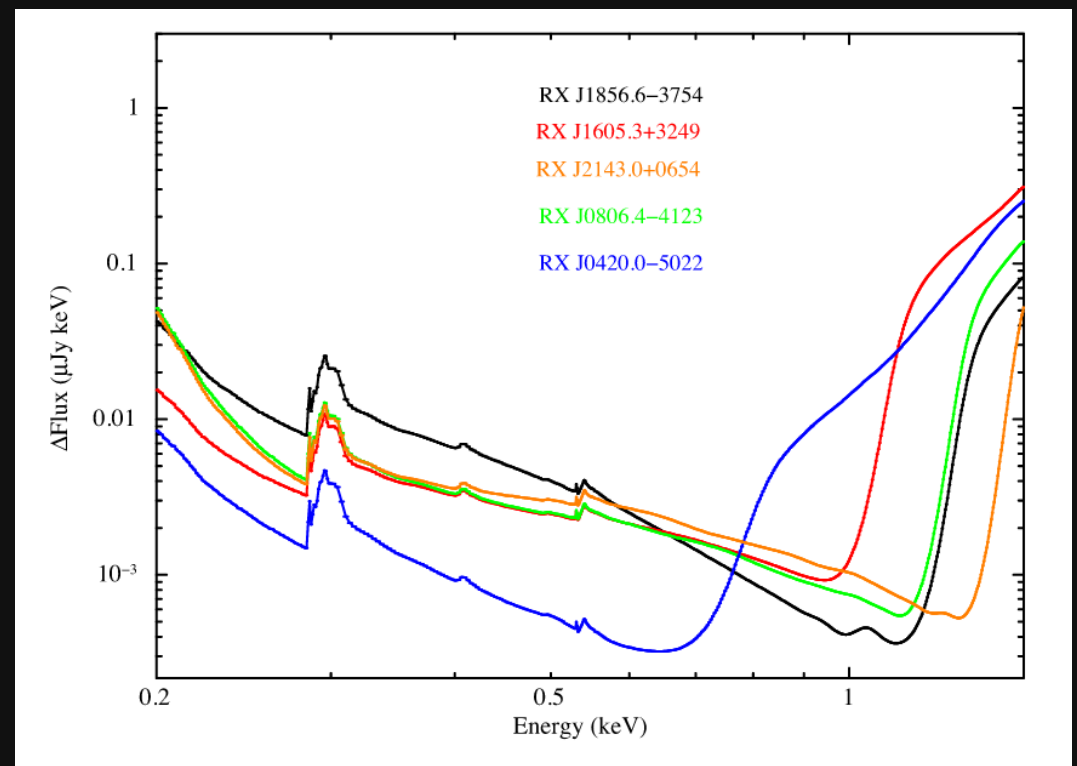
$$\text{Eqw} = 15 \pm 5 \text{ eV}$$



Borghese et al., 2017, MNRAS

3σ upper limits on the equivalent width of a Gaussian line in absorption for the phase-average spectra in the 0.2 - 1.5 keV energy range.

Source	$\sigma_{line} = 0$ (eV)	$\sigma_{line} = 100$ (eV)
RX J1856.5-3754	<10	<14
RX J1605.3+3249	<18	<23
RX J2143.0+0654	<21	<28
RX J0806.4-4123	<32	<69
RX J0420.0-5022	<54	<44



1σ upper limit on a detectable flux variation with respect to the continuum model as a function of energy

CONCLUSIONS

- We searched for narrow phase-dependent absorption features using Energy vs Phase vs Flux diagrams for all XDINSs.
- We discovered two phase-dependent absorption features in two XDINSs.
- Possible origin: proton cyclotron resonant scattering in a small magnetic loop close to the surface.

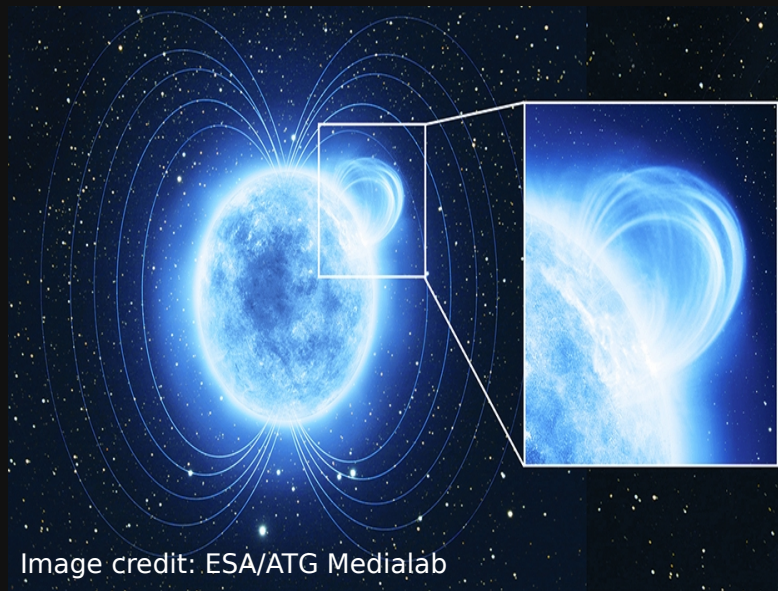


Image credit: ESA/ATG Medialab

$$E_{line} = \frac{eB_{loop}\hbar}{m}$$

$$\left. \begin{array}{l} \text{RX J0720.4-3125} \\ B_{\text{loop}} \approx 1.8 \times 10^{14} \text{ G} \\ B_{\text{dipole}} \approx 2.5 \times 10^{13} \text{ G} \\ \\ \text{RX J1308.6+2127} \\ B_{\text{loop}} \approx 2 \times 10^{14} \text{ G} \\ B_{\text{dipole}} \approx 3.4 \times 10^{13} \text{ G} \end{array} \right\}$$

- Similar lines have been observed in aged magnetars as: SGR0418 & Swift J1822
- These findings strengthen the evolutionary connection between XDINS and magnetars, as well as showing that small magnetic structures close to the NS surfaces might be very common (as expected by theoretical simulations, Obergaulinger et al., 2014).

CONCLUSIONS

- We searched for narrow phase-dependent absorption features using Energy vs Phase vs Flux diagrams for all XDINSs.
- We discovered two phase-dependent absorption features in two XDINSs.
- Possible origin: proton cyclotron resonant scattering in a small magnetic loop close to the surface.



Image credit: ESA/ATG Medialab

$$E_{line} = \frac{eB_{loop}\hbar}{m}$$

$$\left. \begin{array}{l} \text{RX J0720.4-3125} \\ B_{\text{loop}} \approx 1.8 \times 10^{14} \text{ G} \\ B_{\text{dipole}} \approx 2.5 \times 10^{13} \text{ G} \end{array} \right\}$$

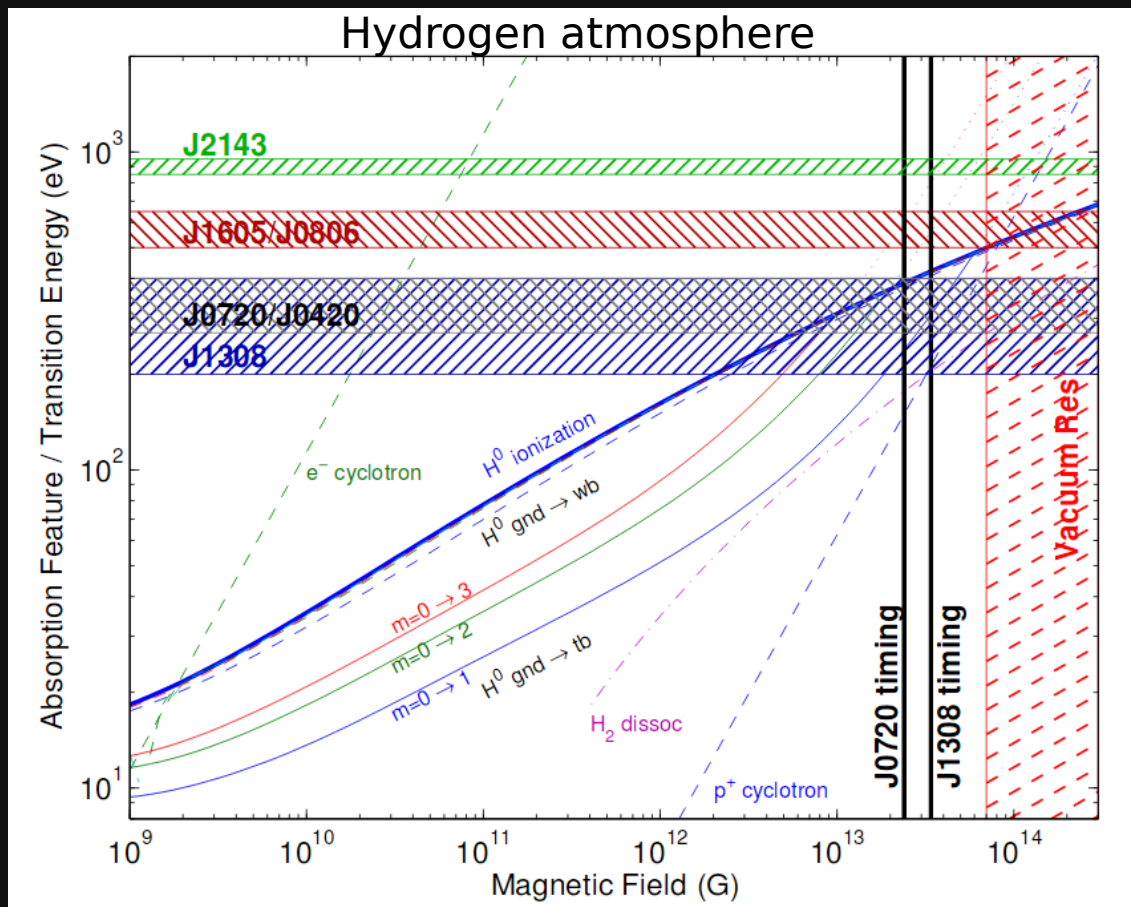
$$\left. \begin{array}{l} \text{RX J1308.6+2127} \\ B_{\text{loop}} \approx 2 \times 10^{14} \text{ G} \\ B_{\text{dipole}} \approx 3.4 \times 10^{13} \text{ G} \end{array} \right\}$$

- Similar lines have been observed in aged magnetars as: SGR0418 & Swift J1822
- These findings strengthen the evolutionary connection between XDINS and magnetars, as well as showing that small magnetic structures close to the NS surfaces might be very common (as expected by theoretical simulations, Obergaulinger et al., 2014).

BACKUP SLIDES

Origin of the broad features:

- 1. proton cyclotron resonances/atomic transitions (van Kerkwijk & Kaplan, 2006)



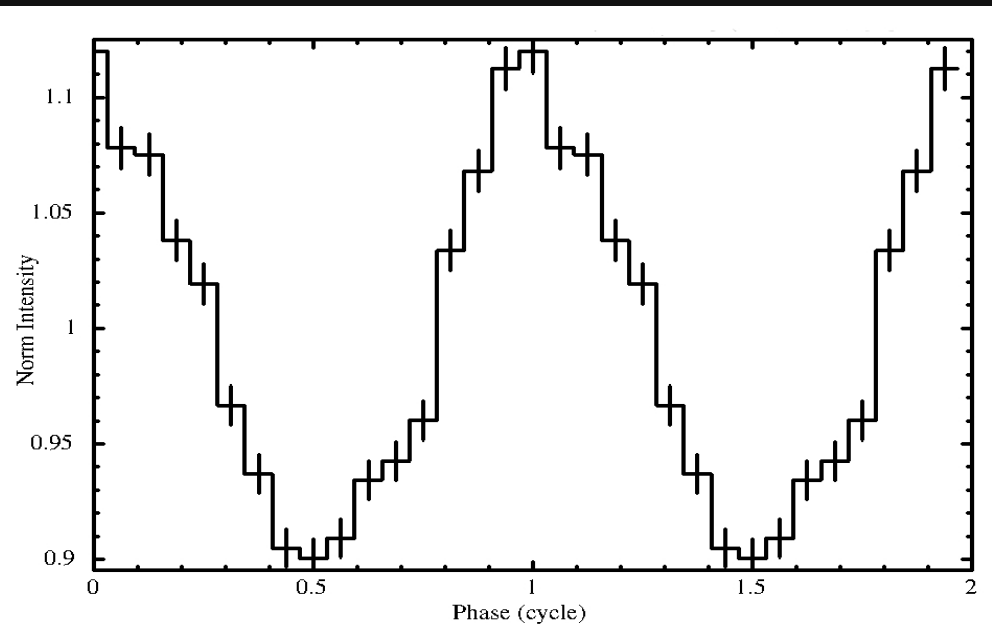
van Kerkwijk and Kaplan, 2007

Helium atmosphere

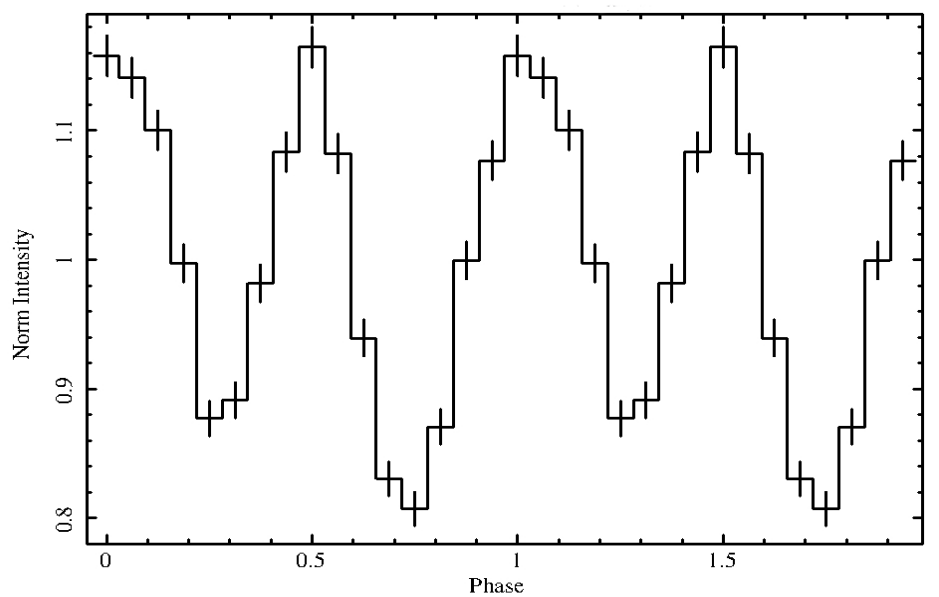
- H burnt in 10^5 yr
- Models predict more than one very strong feature
- Picture incomplete \rightarrow molecules

THE SAMPLE: PULSE PROFILE

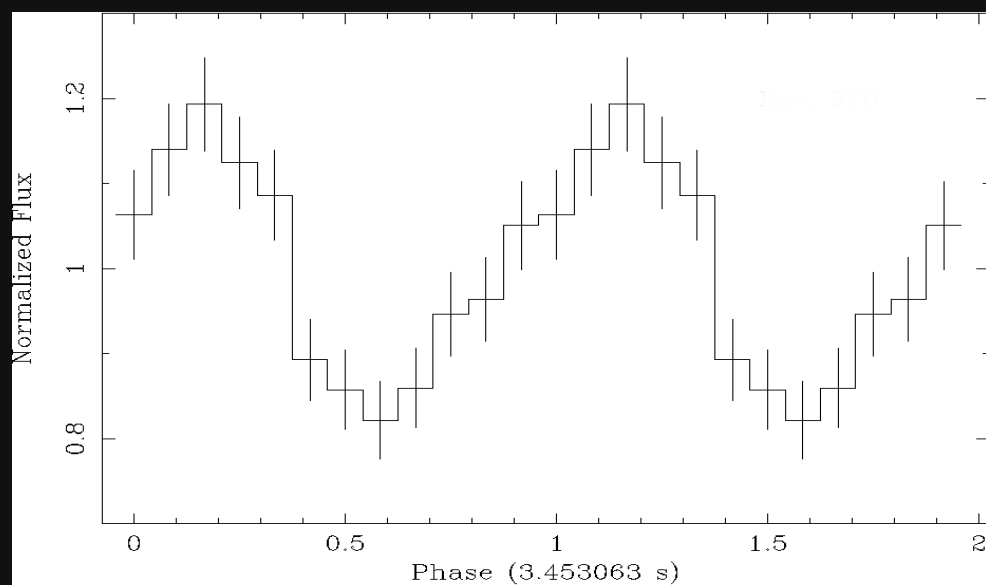
RX J0720.4-3125



RX J1308.6+2127



RX J0420.0-5022



NS ZOO: ABSORPTION FEATURES

PSR J1740+1000

Ordinary rotation-powered radio pulsar

$P = 154 \text{ ms}$, $P_{\text{dot}} = 2.1 \times 10^{-14} \text{ s/s}$, $B = 1.2 \times 10^{12} \text{ G}$

Cyclotron absorption in magnetosphere

XMM observation

RRAT PSR J1819-1458

X-ray counterpart

$P = 4.26 \text{ ms}$, $P_{\text{dot}} = 5.7 \times 10^{-13} \text{ s/s}$, $B = 5 \times 10^{13} \text{ G}$

CCO 1E 1207.4-5209

CCO in SNR 296.5+10.0

First INS to show strong absorption features

$P = 0.424 \text{ s}$, $P_{\text{dot}} = 2.2 \times 10^{-17} \text{ s/s}$, $B = 9.8 \times 10^{10} \text{ G}$

Cyclotron resonant features: electrons ($B=8 \times 10^{10} \text{ G}$) or protons ($B=1.6 \times 10^{14} \text{ G}$)

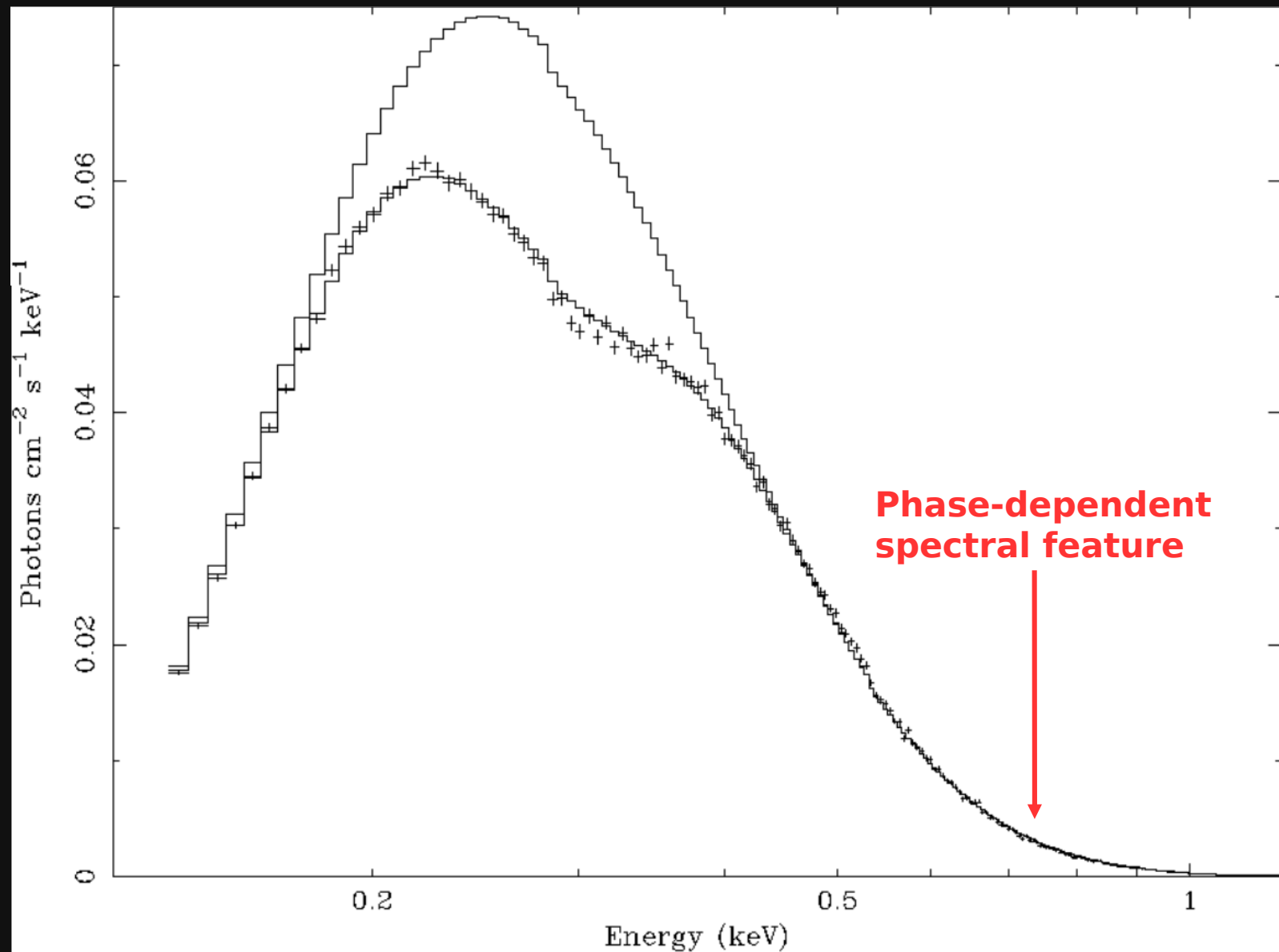
XMM observation (PN+MOS data)

SGR 1806-20

Bursting activity in 1996 - RXTE data

$P = 7.6 \text{ s}$, $P_{\text{dot}} = 2.7 \times 10^{-10} \text{ s/s}$, $B = 1.5 \times 10^{15} \text{ G}$

J0720: PHASE-AVERAGED SPECTRUM



Haberl et al. 2004

TABLE 1
SUMMARY OF THE *XMM-Newton*/EPIC-PN OBSERVATIONS OF RX J0720.4–3125^a

Obs. ID	Obs. Date YYYY-MM-DD	Read-out mode / filter	Live time (ks)	Source net count rate (counts s ⁻¹)	Pile-up fraction ratios $r=0''-30''$
0124100101	2000 May 13	FF / thin	42.8	6.46(1)	0.963(3)
0132520301	2000 Nov 21	FF / medium	22.7	5.60(2)	0.964(4)
0156960201	2002 Nov 06	FF / thin	25.6	6.60(2)	0.969(3)
0156960401	2002 Nov 08	FF / thin	27.1	6.54(2)	0.966(3)
0158360201	2003 May 02	SW / thick	51.0	3.480(8)	1.011(3)
0161960201	2003 Oct 27	SW / thin	12.6	7.52(2)	1.013(5)
0164560501	2004 May 22	FF / thin	32.0	6.96(1)	0.971(3)
0300520201	2005 Apr 28	FF / thin	38.1	6.86(1)	0.968(3)
0300520301	2005 Sep 22	FF / thin	39.1	6.93(1)	0.969(3)
0311590101	2005 Nov 12	FF / thin	33.5	6.75(1)	0.970(3)
0400140301	2006 May 22	FF / thin	17.6	6.83(2)	0.970(4)
0400140401	2006 Nov 05	FF / thin	17.6	6.90(2)	0.966(4)
0502710201	2007 May 05	FF / thin	17.4	6.80(2)	0.968(4)
0502710301	2007 Nov 17	FF / thin	20.1	7.71(2)	0.971(4)
0554510101	2009 Mar 21	FF / thin	16.7	6.84(2)	0.967(4)
0601170301	2009 Sep 22	FF / thin	15.0	6.77(2)	0.968(4)
0650920101	2011 Apr 11	FF / thin	17.6	6.61(2)	0.973(4)
0670700201	2011 May 02	FF / thin	23.6	6.73(2)	0.965(3)
0670700301	2011 Oct 01	FF / thin	22.2	6.60(2)	0.972(3)
0690070201	2012 Sep 18	FF / thin	22.3	6.60(2)	0.970(3)

^a FF: full-frame (time resolution of 73 ms); SW: small window (time resolution of 6 ms). Live time refers to the duration of the observations after filtering for background flares (see text). Count rates refer to the spectra extracted within a circular region with PATTERN = 0. Errors on the count rates are quoted at the 1 σ confidence level. Pile-up fraction ratios were calculated for single events alone and in the 0.1–1.2 keV energy range using the SAS `epatplot` tool.

TABLE 2
PULSE PHASE SPECTROSCOPY FOR MAY, 2ND 2003 OBSERVATION.

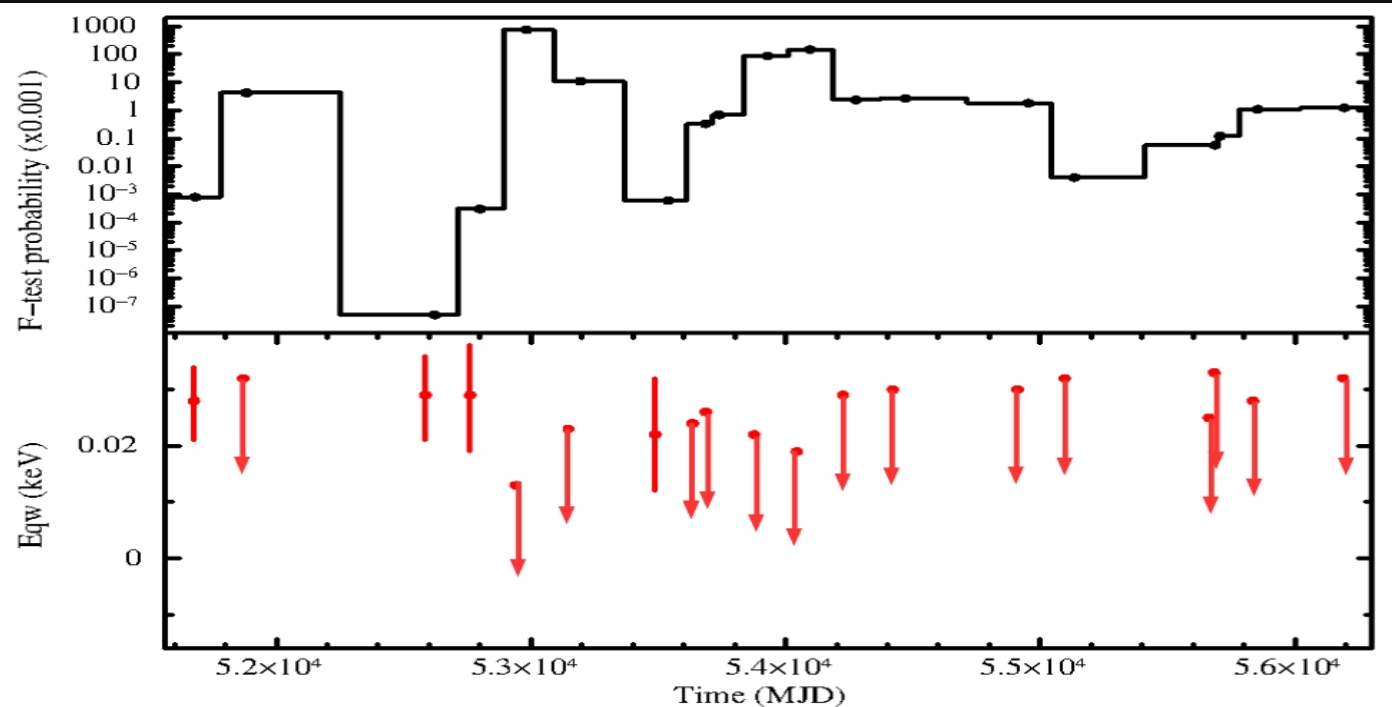
Parameter ^a	0.1–0.3	0.3–0.5	0.5–0.7	0.7–0.9	0.9–1.1
BB					
kT_{BB} (eV)	81.1(6)	81.9(6)	82.2(6)	82.6(6)	82.5(9)
R_{BB} (km)	$6.4^{+0.6}_{-0.5}$	$6.0^{+0.6}_{-0.5}$	$6.1^{+0.6}_{-0.5}$	$6.4^{+0.6}_{-0.5}$	$6.4^{+0.7}_{-0.6}$
Flux ^b	1.16(2)	$1.09^{+0.01}_{-0.02}$	1.14(2)	1.26(2)	1.26(2)
Unabs. Flux ^b	2.20	2.04	2.13	2.34	2.34
NHP	7.2×10^{-2}	5.9×10^{-1}	6.9×10^{-1}	4.2×10^{-2}	2.7×10^{-1}
χ^2_{ν}	1.22	0.96	0.92	1.26	1.09
dof	92	90	92	97	75
BB+GAUSS					
kT_{BB} (eV)	$83.0^{+1.5}_{-0.9}$	82.4(9)	$82.2^{+0.7}_{-0.6}$	82.7(8)	$82.4^{+1.0}_{-0.9}$
R_{BB} (km)	6.0(6)	$6.0^{+0.6}_{-0.5}$	$6.1^{+0.6}_{-0.5}$	$6.3^{+0.6}_{-0.5}$	6.4(6)
$E_{\text{line}}^{\text{c}}$ (eV)	745^{+17}_{-27}	745	745	745	745
$w_{\text{line}}^{\text{c}}$ (eV)	$41.7^{+51.3}_{-33.8}$	41.7	41.7	41.7	41.7
Norm	$9.2^{+3.5}_{-9.2} \times 10^{-5}$	$\leq 2.7 \times 10^{-5}$	$\leq 1.7 \times 10^{-5}$	$\leq 2.9 \times 10^{-5}$	$\leq 2.4 \times 10^{-5}$
Eq. Width (eV)	28^{+9}_{-11}	6^{+9}_{-5}	≤ 8	≤ 11	≤ 13
F-test ^b (10^{-3})	3.5×10^{-7}	232	1000	750	>1000
NHP	7.9×10^{-1}	6.0×10^{-1}	6.6×10^{-1}	3.6×10^{-2}	2.5×10^{-1}
χ^2_{ν}	0.88	0.95	0.93	1.27	1.11
dof	89	89	91	96	74

^a N_{H} was frozen at the value obtained for the phase averaged spectra: $N_{\text{H}} = 1.9 \times 10^{20} \text{ cm}^{-2}$.

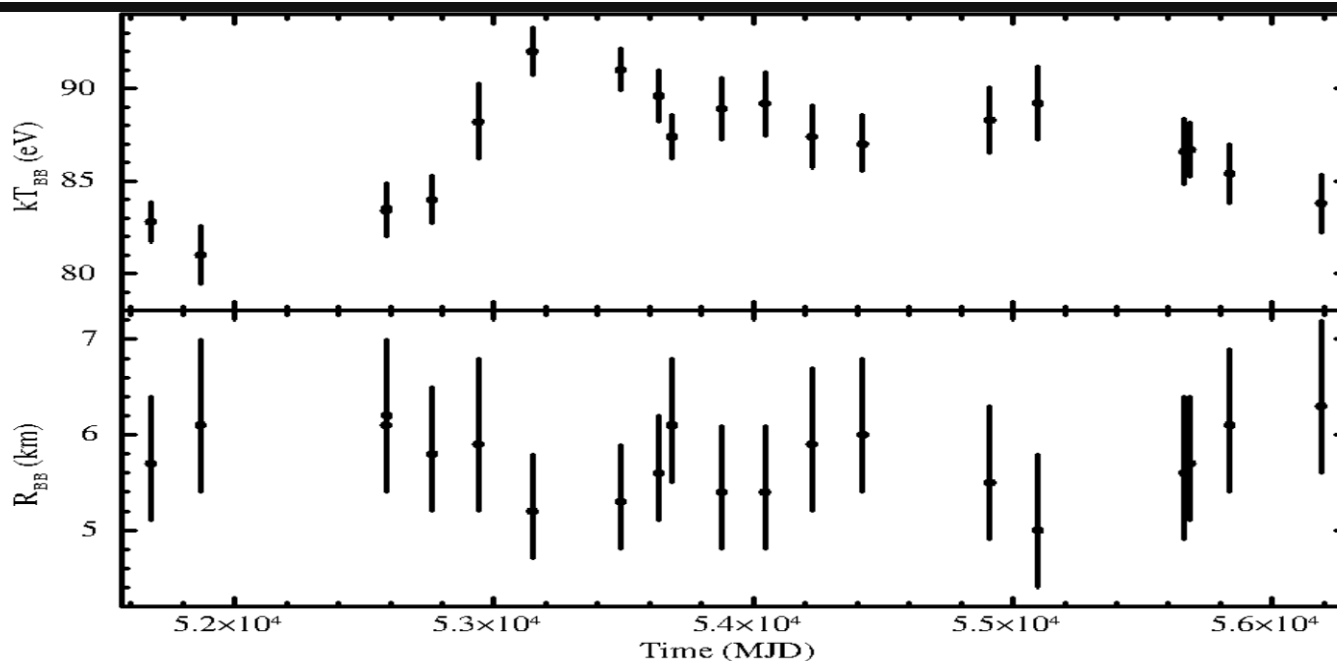
^b Fluxes are calculated in the 0.1–2 keV energy range, and in units of ($10^{-11} \text{ ergs}^{-1} \text{cm}^{-2}$)

^c Line energy and width were frozen at the value obtained for the phase interval 0.1 – 0.3: $E_{\text{line}} = 745 \text{ eV}$ and $\sigma = 42 \text{ eV}$.

J0720: PHASE-DEPENDENT FEATURE IN ALL XMM-Newton OBS



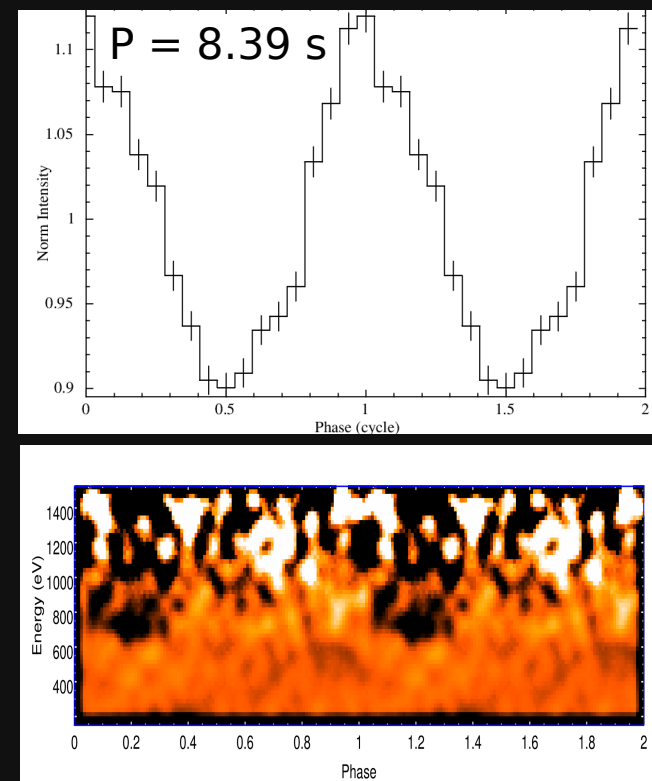
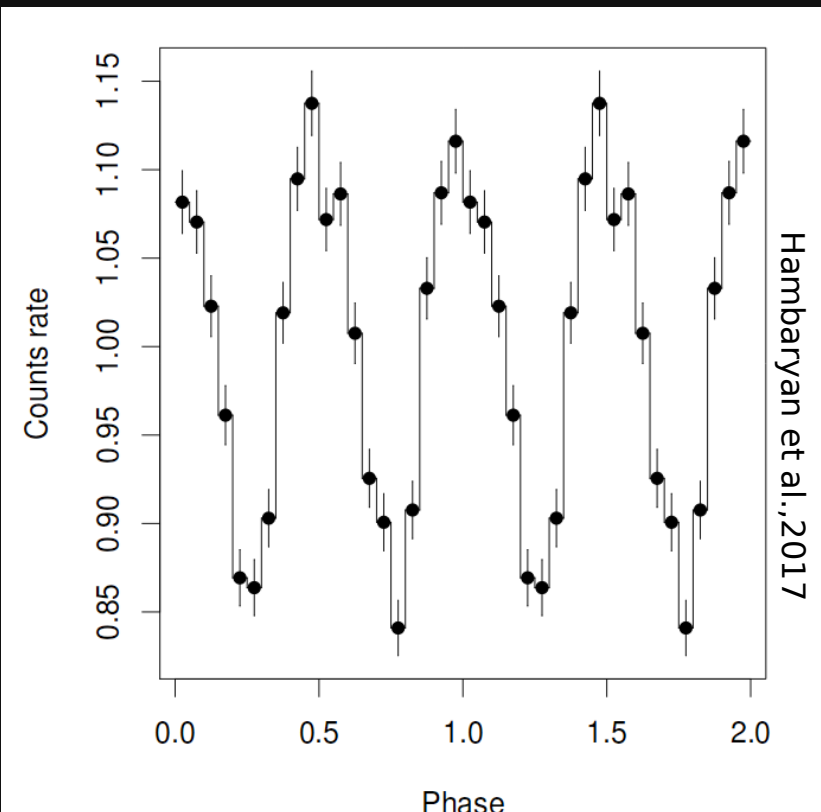
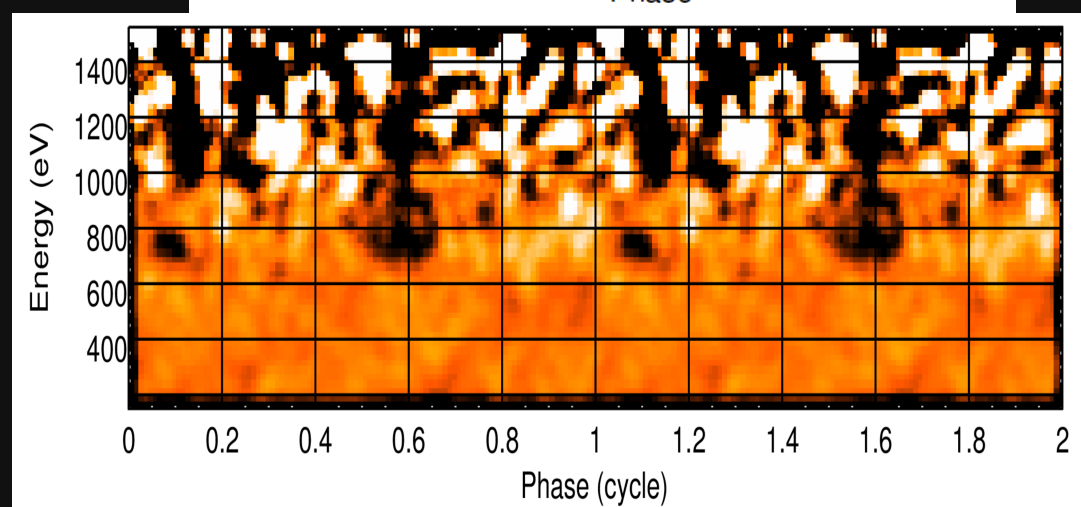
F-test probability and
Eqw as a function of
time for the phase-
resolved spectra in the
0.1-0.3 phase range



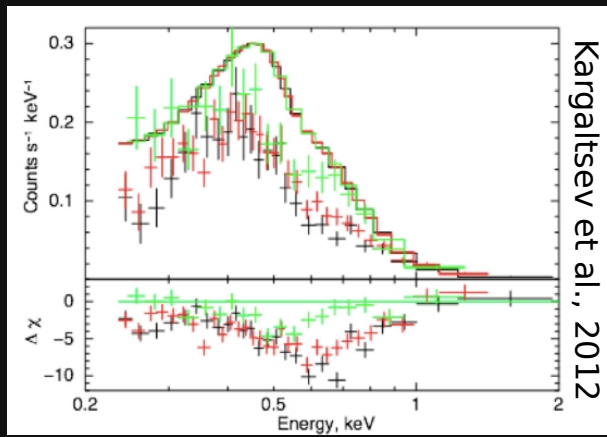
Temporal evolution of BB
parameters for all the
phase-averaged spectra

RX J0720.4-3125: new period?

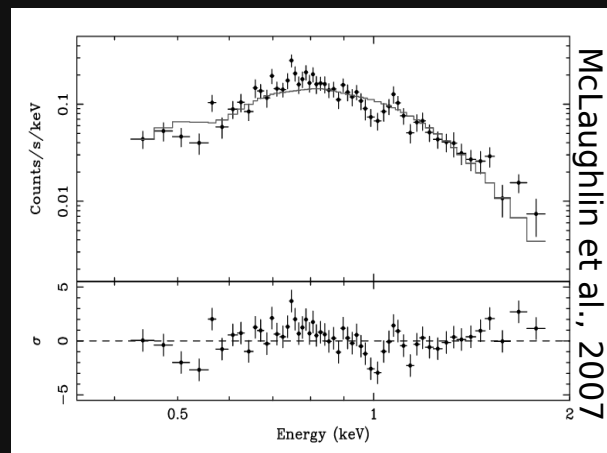
$P_{\text{new}} = 16.78 \text{ s}$



PSR J1740+1000
 $E_{\text{line}} \sim 0.6 \text{ keV}$

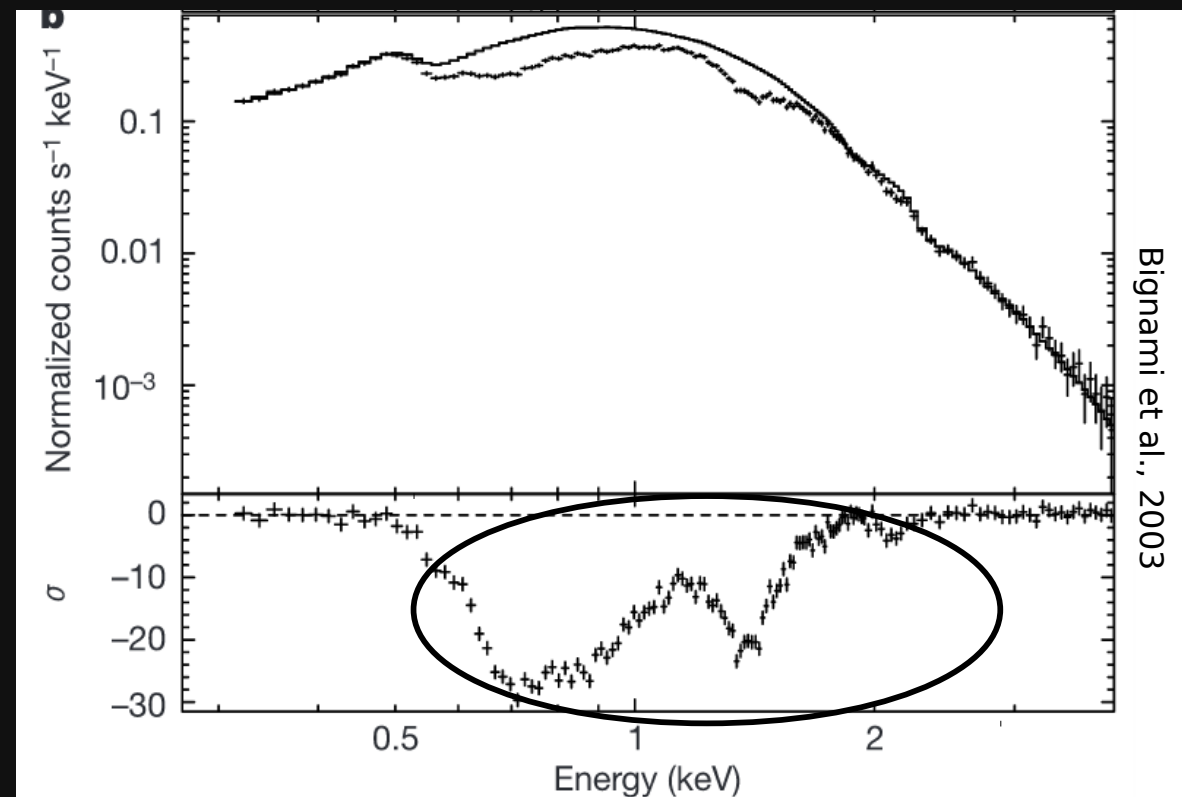


RRAT PSR J1819-1458
 $E_{\text{line}} \sim 1 \text{ keV}$



CCO

1E 1207.4-5209
 $E_{\text{line}} \sim 0.7, 1.4, 2.1 \text{ keV}$



POSSIBLE INTERPRETATIONS

- atomic transition in a magnetized atmosphere

Presence of an atmosphere not supported by the observations

Composition: He or mid-Z elements

Phase dependence → reprocessing in a limited region

Small hot spots



broad pulse profile
large radiation radius

Atmosphere with a clumpy
structure only on small part



How ?